



HAL
open science

Possible identification of local deposits of Cl_2SO_2 on Io from NIMS/Galileo spectra

B. Schmitt, C. Sotin, R. Jaumann, B. Buratti, R. Brown, R. Clark, L.
Soderblom, K. Baines, G. Bellucci, J.-P. Bibring, et al.

► To cite this version:

B. Schmitt, C. Sotin, R. Jaumann, B. Buratti, R. Brown, et al.. Possible identification of local deposits of Cl_2SO_2 on Io from NIMS/Galileo spectra. *Journal of Geophysical Research, American Geophysical Union*, 2003, 108 (E9), pp.8-1-8-19. 10.1029/2002JE001988 . hal-03657548

HAL Id: hal-03657548

<https://hal-univ-paris.archives-ouvertes.fr/hal-03657548>

Submitted on 25 Jun 2022

HAL is a multi-disciplinary open access archive for the deposit and dissemination of scientific research documents, whether they are published or not. The documents may come from teaching and research institutions in France or abroad, or from public or private research centers.

L'archive ouverte pluridisciplinaire **HAL**, est destinée au dépôt et à la diffusion de documents scientifiques de niveau recherche, publiés ou non, émanant des établissements d'enseignement et de recherche français ou étrangers, des laboratoires publics ou privés.

Copyright

Possible identification of local deposits of Cl₂SO₂ on Io from NIMS/Galileo spectra

B. Schmitt

Laboratoire de Planétologie de Grenoble, CNRS-Université J. Fourier, Saint Martin d'Hères, France

S. Rodriguez

Observatoire de Bordeaux, Floirac, France

Received 30 September 2002; revised 16 May 2003; accepted 23 May 2003; published 6 September 2003.

[1] Starting from the recent discovery of chlorine ions in Io's plasma torus, we searched for evidence of Cl-bearing species at the surface of the satellite. We have identified Cl₂SO₂, with possible contribution by ClSO₂, as candidates for the absorber(s) of the 3.92 μm band locally present in NIMS/Galileo spectra of the reddish deposits south of Marduk's volcanic center. Low-temperature laboratory measurements of the infrared spectra of several Cl and S-bearing molecules in the solid state, coupled with radiative transfer modeling, first allowed us to select four candidate molecules. Their abundance and stability at Io's surface have been tested through formation, condensation, and destruction scenarios using volcanic and atmospheric models completed with chemical and thermodynamical data. In particular, the sublimation rates of solid Cl₂SO₂ and SO₂ have been measured to study the selective condensation of these species. Cl₂SO₂ diluted at ~1% in a millimeter thick layer of solid SO₂ is the favorite candidate for the 3.92 μm band. We strongly favor a formation process of this molecule by heterogeneous reaction of Cl atoms on SO₂ ice condensing on plume particles or at Io's surface. The high Cl₂SO₂ abundance observed implies that a Cl-rich volcanic eruption ($[\text{Cl} - (\text{Na} + \text{K})]/\text{S} > 0.015$) occurred at Marduk. ClSO₂ is a potential additional contributor to the band. Pure H₂S is safely discarded as it is extremely unstable at Io's surface but an upper limit of 0.01% is derived for H₂S diluted in SO₂. Finally, chemical constraints allow us to firmly exclude H₂S₂. We also suggest that Cl₂S may be an alternative explanation for the reddish coloration of some volcanic deposits. *INDEX TERMS*: 5410 Planetology: Solid Surface Planets: Composition; 5470 Planetology: Solid Surface Planets: Surface materials and properties; 5480 Planetology: Solid Surface Planets: Volcanism (8450); 6218 Planetology: Solar System Objects: Jovian satellites; 3934 Mineral Physics: Optical, infrared, and Raman spectroscopy; *KEYWORDS*: Io's surface composition, chlorine chemistry, Cl₂SO₂, H₂S, infrared spectroscopy, NIMS-Galileo spectra

Citation: Schmitt, B., and S. Rodriguez, Possible identification of local deposits of Cl₂SO₂ on Io from NIMS/Galileo spectra, *J. Geophys. Res.*, 108(E9), 5104, doi:10.1029/2002JE001988, 2003.

1. Introduction

[2] Since 1979 SO₂ is the only molecule firmly identified at the surface of Io [Smythe *et al.*, 1979; Fanale *et al.*, 1979; Hapke, 1979]. Most of the numerous features observed in Io's spectra were attributed to this species by comparison with laboratory data from the midinfrared to the ultraviolet thus confirming without ambiguity its identification [Nash *et al.*, 1980; Howell *et al.*, 1989; Schmitt *et al.*, 1994, manuscript in preparation, 2003; Carlson *et al.*, 1997]. Several forms of allotropic sulfur (S₂, S₄, and S₈), S₂O and polysulfur oxides could explain some spectral features of Io's visible spectra [Moses and Nash, 1991; Hapke,

1989] and are strongly suspected at the satellite surface. Laboratory measurements have shown that SO₂ and S₈ could also explain two of the emission features seen in the midinfrared spectra recorded by the IRIS/Voyager 1 instrument [Hanel *et al.*, 1992; Pearl, 1988]. Detailed Galileo data analysis has shown that SO₂ and sulfur allotropes are dominant compounds of the chemical composition over most of the satellite surface [Geissler *et al.*, 1999; Douté *et al.*, 2001]. A few other molecules have been suggested to explain some of the remaining absorption and emission bands seen on Io's spectra. In the Iris spectra frozen SO₃ was also proposed by Khanna *et al.* [1995] to contribute to the two bands previously assigned to SO₂ and S₈. However, their laboratory near-infrared spectra of SO₃ showed features around 4.03–4.08 μm which were not seen in the observational data. A weak 3.91 μm band observed on the

side of the strong 4.07 μm band of solid SO₂ was first attributed to H₂S, either pure [Nash and Howell, 1989] or diluted in SO₂ [Salama et al., 1990], but Schmitt et al. [1994, manuscript in preparation, 2003] showed that solid SO₂ could fully explain this feature. Schmitt et al. also reattributed to SO₂ two other near-infrared bands formerly explained by H₂S [Lester et al., 1992] and CO₂ [Sandford et al., 1991]. The possible identification of H₂O [Salama et al., 1994] met with the same fate [Dahmani and Khanna, 1996; Nash and Betts, 1998; B. Schmitt et al., manuscript in preparation, 2003]. Sodium and potassium have been also suspected to be present in some solid form because they were discovered in Io's torus [Brown, 1974]. The possible contribution of Na₂S, NaHS, K₂S, Na₂SO₃, and Na₂SO₄ to Io's reflectance spectrum has been studied [Nash and Nelson, 1979; Nash, 1988; Howell et al., 1989] but none has been yet positively identified at the surface. The net result of these spectral studies is that there is either no or still controversial identifications to all the bands not attributed to SO₂, the only molecule unquestionably condensed on Io's surface.

[3] The recent discovery of abundant chlorine ions in Io's plasma torus [Küppers and Schneider, 2000; Feldman et al., 2001] led us to consider a new family of candidates to explain some of the unidentified or controversial features of Io's surface spectra: Cl-bearing molecules. On the basis of Io's torus atomic abundances, a large number of molecules composed of S, O, Na, K, Cl, and H are predicted in Io's atmosphere by Zolotov and Fegley [1998a] and Fegley and Zolotov [2000] as the result of lava degassing and high temperature volcanic chemistry. Thirteen of the molecules predicted by Zolotov and Fegley [1998a] contain chlorine; therefore it is probable that some of these Cl-bearing species could be found at the surface of the satellite.

[4] Although they are not the dominant Cl compounds predicted by the chemical model under most of the physical conditions studied, we first decided to study the four infrared-active and commercially available molecules containing at least one Cl and one S atom: Cl₂S, Cl₂S₂, Cl₂SO and Cl₂SO₂ (S. Rodriguez and B. Schmitt, Infrared spectra of chlorine-sulfur bearing species as pure solids and diluted in SO₂ ice: Implications for Io's surface composition, submitted to *Planetary and Space Sciences*, 2003) (hereinafter referred to as Rodriguez and Schmitt, submitted manuscript, 2003). No infrared spectrum is available in the literature for these four molecules in the solid state. Only gas phase or rare gas matrix IR spectra or liquid Raman spectra exist [Schinanouchi, 2000]. We also performed specific laboratory experiments on two "classical" candidates, H₂S and SO₃, for which a few solid state spectra have already been published [Reding and Hornig, 1957; Ferraro et al., 1980; Salama et al., 1990; Nelson and Smythe, 1986; Khanna et al., 1995].

[5] In this paper we focus on the analysis of one new infrared absorption band at 3.920 μm we recently discovered locally in NIMS/Galileo spectro-images of Io [Schmitt and Rodriguez, 2000; Schmitt et al., 2001]. We will only describe the spectroscopic experiments with Cl₂SO₂ and H₂S necessary for the identification of this band. We will also present some sublimation experiments of SO₂ and Cl₂SO₂ designed to determine their relative volatility. The detailed presentation of the laboratory experiments on the

six molecules listed above will be published in future papers (see Rodriguez and Schmitt (submitted manuscript, 2003) for the Cl-bearing molecules).

2. Observational Data

[6] The Io observations collected by the Galileo NIMS instrument cover the 0.7–5.2 μm range at 0.025 μm resolution [Carlson et al., 1992]. From these observations the only compound clearly identified so far at its surface is SO₂ (from a series of 8 absorption bands [Carlson et al., 1997]). A few other weaker absorption features widely distributed on Io have been observed [Carlson et al., 1997; Soderblom et al., 1999] but are still awaiting identification. During a systematic search a spectral absorption feature at 3.920 \pm 0.005 μm appeared to be locally present in a few groups of pixels of the full spectral resolution data (INHRSPEC) acquired during the G2, C3, E4, E6, G7 and E14 orbits (September, November and December 1996, February and March 1997, March 1998) and caught our attention.

[7] We concentrated on the G2 data which have the best signal-to-noise ratio. After a careful check in the raw G2 data (i.e., detector pixels before spectral/geometrical reprojection) for possible energetic particle spikes, the occurrence of this band has been clearly confirmed in at least one area south of Marduk (centered around 31°S, 209°W). Only the 3.955 μm channel was found to be partly affected by a "positive spike" in one detector pixel adjacent to the three detector pixels displaying the band. The spatial reprojection in Io geographic coordinates propagated part of this spike into some of the "end-product" pixels showing the 3.920 μm band. A deconvolution and despiking procedure of the spectra has been developed by Soderblom et al. [1999] and applied to the data of the G2 orbit. The resulting spectra around Marduk are much less noisy and well corrected from the spike near the 3.920 μm band. The average deconvolved reflectance spectrum of this region (five reprojected pixels covering about 350 \times 270 km²) measured during the G2 orbit is plotted in Figure 1 and compared to an average spectrum of a nearby area showing only SO₂ ice bands. The mean incidence, emergence, and phase angles of the averaged south Marduk observations are 31.5°, 33°, and 1.50°, respectively. The location of the pixels displaying the band are drawn on the SSI context image of the Marduk region (Figure 2). Spatial coregistration between NIMS G2 and SSI data are accurate within $\pm 1^\circ$ (latitude and longitude).

[8] The independent observation of the band, but at lower signal to noise, covering about the same area (within NIMS pointing accuracy) in the E4, G7 and E14 data strengthens its occurrence. In particular in the E4 observation, recorded at higher spatial resolution than G2, the feature covers 8 contiguous pixels. Unfortunately the highest spatial resolution data, C3, are too noisy to firmly confirm the occurrence of the band. In the E6 data a few pixels near Marduk display the band but are shifted by about 6° in longitude, possibly due to a registration problem. In summary, within the above limitations, the available set of NIMS observations consistently displays the 3.920 μm band with similar intensities in the region south of Marduk.

[9] It should be noted that the $\nu_1 + \nu_3$ band of SO₂ (4.07 μm) has a wide "side-plateau" with small bumps in

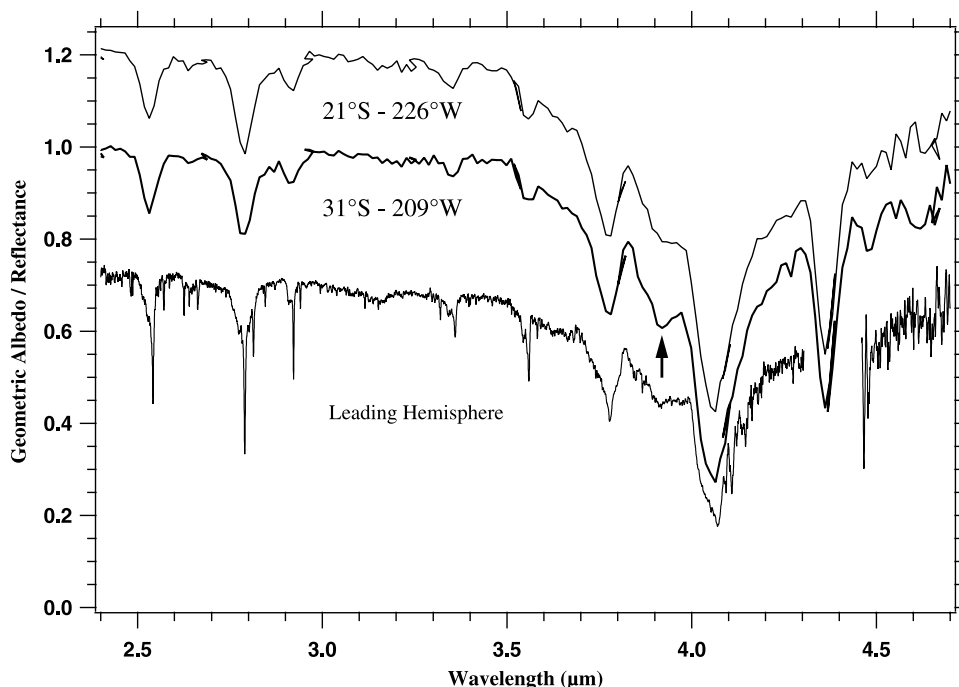


Figure 1. The NIMS average reflectance spectrum (middle curve) south of Marduk (G2 orbit, center $\sim 31^\circ\text{S}$, 209°W ; see Figure 2 for exact location) displaying the $3.920\ \mu\text{m}$ band (arrow) compared to an average spectrum of a nearby area showing only SO_2 ice bands (centered 21°S – 226°W ; top curve with vertical shift: $+0.15$). The ISO leading hemisphere spectrum of Io (Geometric albedo; bottom curve with vert. shift: -0.05) is also shown at full spectral resolution as a “pure SO_2 ice” reference in this range (B. Schmitt et al., manuscript in preparation, 2003). Note in this spectrum the weak SO_2 band at $3.92\ \mu\text{m}$ formerly attributed to H_2S on Io.

the 3.85 – $4.0\ \mu\text{m}$ range corresponding to combinations with phonon modes [Schmitt et al., 1994] that are easily observed in high spectral resolution full disk spectra (B. Schmitt et al., manuscript in preparation, 2003) (see Figure 1). They are these bumps that have been formerly attributed to pure solid H_2S [Nash and Howell, 1989] or diluted in SO_2 [Salama et al., 1990]. The band at $3.920\ \mu\text{m}$ we observe in the NIMS spectra is much stronger and is superimposed on the SO_2 “bumpy plateau.” The depth of the $3.920\ \mu\text{m}$ band relative to this “ SO_2 continuum” is about 5%.

3. Laboratory Measurements

[10] Laboratory transmission spectra in the midinfrared (1.5 – $25\ \mu\text{m}$) were obtained on thin films at $1\ \text{cm}^{-1}$ resolution with our Fourier transform infrared spectrometer (Nicolet 800) fitted out with an ultra-high vacuum cryogenic optical cell. A brief description of the experimental setup and procedure can be found in Schmitt et al. [1994]. Thin films of solid Cl_2SO_2 (sulfuryl chloride), H_2S and SO_2 samples were synthesized in the vacuum optical cell by the technique of direct gas deposition on a CsI window.

[11] We performed experiments on pure solid samples as well as for these molecules diluted in solid SO_2 (Figure 3). Gas phase spectra were also recorded for reference.

3.1. Cl_2SO_2 Spectra

[12] Several successive deposits of pure Cl_2SO_2 gas (liquid purity $>99\%$) were made at $120\ \text{K}$ (2 – $15\ \mu\text{m}$ thick),

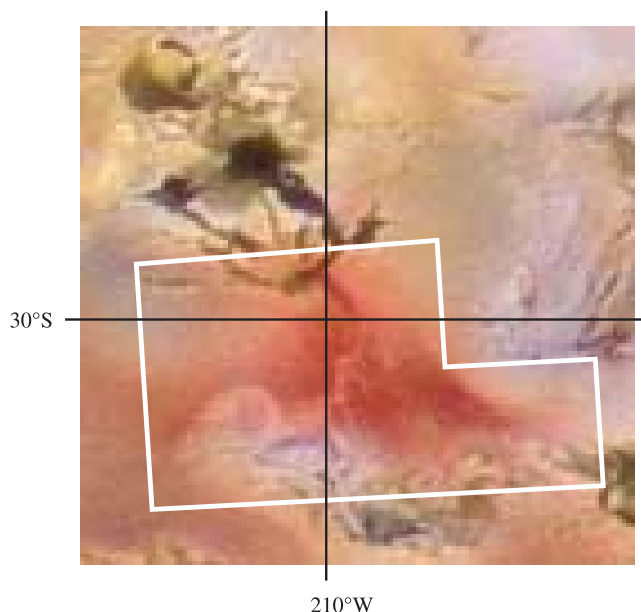


Figure 2. SSI context image of the Marduk region (cylindrical projection) [McEwen et al., 1998]. The image size is about 15° in longitude and 17° in latitude ($420 \times 540\ \text{km}$). The location of the group of five NIMS G2 pixels clearly displaying a $3.920\ \mu\text{m}$ band is shown as a white box. Note the good correlation with the red deposits.

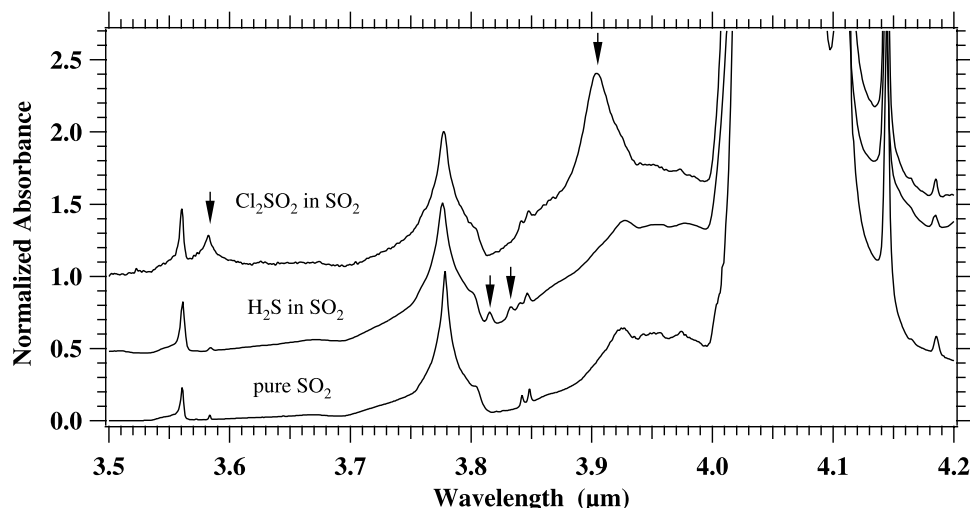


Figure 3. Laboratory absorbance spectra of solid mixtures of 2% Cl_2SO_2 in SO_2 (100 K) and 2.8% H_2S in SO_2 (130 K) compared to pure SO_2 ice (125 K). The curves are offset by 0.5 unit for clarity. The arrows show the location of the Cl_2SO_2 and H_2S bands.

then cooled to 100 K and slowly warmed by steps of 10 K until complete sublimation of the sample occurred around 160 K. After each deposit and each temperature step we recorded a mid-IR transmission spectrum of the sample. For the study of Cl_2SO_2 diluted in SO_2 , a gas mixture of 2.0% of Cl_2SO_2 in SO_2 (SO_2 gas purity >99.9%) was first prepared in a glass bulb, then sent to the deposition tube of the optical cell and cocondensed in several steps on the infrared window at 100 K (thickness increasing from 0.5 to 185 μm with condensation rates from 1 to 160 $\mu\text{m h}^{-1}$). This lower temperature was chosen because of the higher volatility of SO_2 . The resulting solid sample was homogeneously and intimately mixed. Transmission spectra were also acquired with the same procedure until the sample totally sublimated (first SO_2 around 130–140 K, then Cl_2SO_2 around 160 K).

[13] Between 2.5 and 25 μm , we observe about 25 absorption bands of various intensities and attribute them to 7 fundamental vibration modes of Cl_2SO_2 , 10 combination modes (with only three below 5 μm : $2\nu_1$, $\nu_1 + \nu_6$, and $2\nu_6$), and several isotopic bands (mainly from ^{37}Cl and ^{34}S) (Rodriguez and Schmitt, submitted manuscript, 2003).

[14] The wavelength shifts between the band positions of the pure solid state and diluted state occur in both directions and range from weak to medium depending on the vibration mode. In particular the $\nu_1 + \nu_6$ combination mode measured at 3.9015 μm at 120 K in the pure solid state shifts to 3.9075 μm upon dilution in SO_2 at the same temperature. The position of this band is found to be strongly temperature sensitive in the diluted state (-0.2 nm K^{-1}) in comparison with the 15 times weaker sensitivity measured for pure Cl_2SO_2 . There are also strong changes in the relative band intensities. This is particularly the case for the three combination modes of ν_1 and ν_6 : with similar intensities for pure Cl_2SO_2 , the $\nu_1 + \nu_6$ mode becomes markedly predominant when diluted in solid SO_2 (Figures 3 and 4). The $2\nu_1$ mode near 4.25 μm is then barely distinguishable in the wing of

the SO_2 band. Consequently, the Cl_2SO_2 band positions and intensities are relevant indicators of the physical state (temperature and dilution state) of this molecule.

[15] We extracted the absorption coefficient of diluted Cl_2SO_2 and normalized it to the density of pure Cl_2SO_2 using a procedure and assumptions similar to the ones described by *Quirico et al.* [1999] for CH_4 diluted in N_2 . The main difference is that the SO_2 absorptions strongly dominate the spectrum making their subtraction more difficult. The spectrum was normalized assuming that the molar integrated absorption coefficient of the $\nu_1 + \nu_6$ band is the same for pure and diluted Cl_2SO_2 . A density of $2.36 \pm 0.35 \text{ g cm}^{-3}$ and a corresponding refractive index of 1.675 ± 0.12 were also assumed for pure solid Cl_2SO_2 (see the Cl_2SO_2 sublimation section). With these assumptions the derived absorption coefficient spectrum is fully consistent with the values directly obtained using the thickness of the sample (185 μm) and the nominal concentration (2.0%) of the condensed $\text{Cl}_2\text{SO}_2:\text{SO}_2$ gas mixture.

3.2. H_2S Spectra

[16] Two pure H_2S samples (gas purity >99.7%) were condensed at temperatures of 15 and 80 K. Mid-IR spectra were recorded during step warmup to 90 K where H_2S rapidly sublimates under vacuum. In order to also obtain spectra at a temperature more relevant to daytime temperatures on Io we designed an experiment in which the sample is condensed and dynamically stabilized at 107 K by continuing deposition at a rate adjusted to compensate sublimation losses. Mid and near-IR spectra of H_2S mixed in SO_2 have been also studied several years ago with a SO_2 sample condensed with 2.8% H_2S and 4.7% CO_2 [Schmitt *et al.*, 1994, 1998].

[17] The two strong and closely spaced stretching fundamental modes ν_1 and ν_3 dominate the 3–5 μm spectrum of H_2S . Their absorption bands strongly change with temperature due to the occurrence of three different crystalline phases in the 80–130 K range [Anderson *et al.*, 1977]. Below 103.6 K the ordered phase III displays three sharp bands at 3.923 μm (ν_3 mode), 3.941 and 3.957 μm (both ν_1

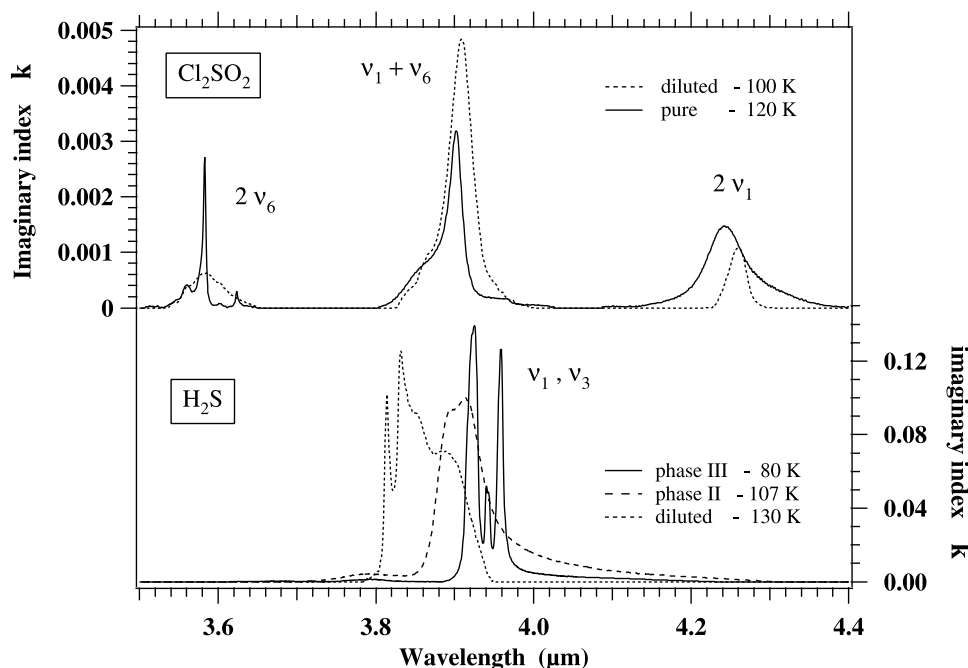


Figure 4. Imaginary refractive index (k) spectra of Cl_2SO_2 and H_2S in the 3.5–4.4 μm region. Upper part: pure Cl_2SO_2 and diluted in SO_2 . Lower part: two crystalline phases of pure H_2S and diluted in SO_2 . For the diluted molecules the index is normalized to the density of the pure solids after subtraction of the absorption of the SO_2 matrix.

mode) while the disordered phase II (below 126.2 K) has only one broad structured band centered around 3.906 μm (Figure 4). At higher temperatures phase I is reported to display a very similar, although slightly narrower, single band at 3.910 μm [Reding and Hornig, 1957]. All these bands are only very slightly temperature sensitive, within a given crystalline phase. A few much weaker bands also occur between 1.93 and 2.0 μm .

[18] The spectrum of H_2S mixed in SO_2 has also a clearly different shape with a series of blended bands strongly shifted (by more than 0.08 μm) relative to pure H_2S . Figure 4 shows the monomer and multimer absorption bands of H_2S at 110 K after the removal of the contribution of the SO_2 matrix, which strongly absorb in that range (Figure 3). When H_2S is diluted at lower concentrations (i.e., $\ll 1\%$) only the two sharp monomer bands at 3.814 (ν_3 mode) and 3.831 μm (ν_1 mode) remain, a result consistent with the measurements of Salama *et al.* [1990] at 85–100 K, but not with their mode attribution. All these spectral changes allow us to easily distinguish the different phases and to set temperature limits.

[19] The absorption coefficient of the disordered phase II H_2S at 107 K was obtained by assuming that the integrated absorption coefficient of the 3.906 μm band is the same as for amorphous (15 K) H_2S . This assumption was necessary because we were not able to monitor the effective (and changing) thickness of the high temperature samples (>80 K) in this dynamic experiment. The extraction protocol of the absorption coefficient of H_2S diluted in SO_2 was about the same as for Cl_2SO_2 .

3.3. Sublimation Rates

[20] Experiments were performed to measure the sublimation rate of pure solid SO_2 and Cl_2SO_2 at low temperature

in order to estimate their temperature dependent vapor pressure curves.

3.3.1. SO_2 Sublimation

[21] For solid SO_2 a sample about 80 μm thick was slowly condensed at 110 K. Its deposition rate and thickness were monitored by He-Ne laser interferences and by recording several near-infrared spectra. After condensation a near-infrared spectrum was recorded before warmup to 120 K where the sample was allowed to sublimate. The temperature is stabilized within ± 0.05 K and its absolute value at the sample surface is known within ± 0.2 K. The residual SO_2 pressure in the constantly pumped cell was about $6 (\pm 2) \times 10^{-10}$ bar during the 14.5 hours necessary for complete sublimation of the sample. Spectra were recorded during sublimation. The thicknesses x were determined from the spectral interference fringes in the 3.0–3.7 μm and 4.5–5.2 μm “continuum” ranges ($x = 1/(2n_\nu \Delta\nu)$ for normal incidence, where n_ν is the refractive index at wavenumber ν and $\Delta\nu$ is the wavenumber period of the spectral interference). The occurrence of these spectral fringes demonstrates a high homogeneity of the sample thickness (better than 0.5%) within the measurement area. The refractive index of solid SO_2 has been previously estimated from the Lorenz-Lorentz equation to be 1.50 ± 0.03 at 0.633 μm [Schmitt *et al.*, 1994]. Taking into account the dispersion of the refractive index (estimated from Kramers-Kronig relation [Trotta, 1996]), we obtain a value of $n \approx 1.46 \pm 0.04$ in the 3–5 μm range where the fringes have been measured.

[22] A sublimation rate of $1.50 (\pm 0.04) \times 10^{-3} \mu\text{m s}^{-1}$ at 120.0 ± 0.2 K was determined by this technique. This value is consistent to within 1% with the rate calculated using the initial thickness determined with the He-Ne laser interferences during deposition. On the other hand it is 5.5 times

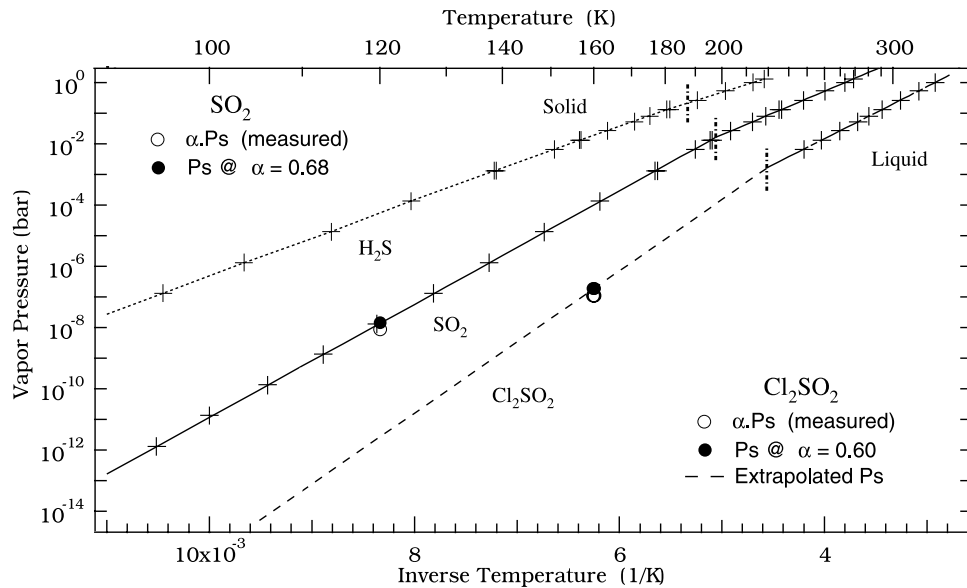


Figure 5. Saturation vapor pressure of H_2S , SO_2 and Cl_2SO_2 as a function of temperature. Data for solid and liquid H_2S and SO_2 (crosses) are from *Honig and Hook* [1960]. Our sublimation rate measurement of SO_2 ice at 120 K (circle) is consistent with the SO_2 curve with a condensation coefficient $\alpha \approx 0.68 \pm 0.15$ (dot). Data for liquid Cl_2SO_2 are from *Lide* [1990]. The vapor pressure curve of solid Cl_2SO_2 (dashed line) is obtained by fitting a thermodynamic law to our data at 160 K (dot; assuming $\alpha \approx 0.60$) and to the saturation pressure at the triple point.

larger than the nominal value calculated at 120 K from the sublimation equation of SO_2 derived by *Sandford and Allamandola* [1993].

[23] From statistical thermodynamics [see, e.g., *Haynes et al.*, 1992],

$$\frac{dx}{dt} = \frac{M}{\rho(T)} \frac{\alpha(T)(P_s(T) - P_g)}{\sqrt{2\pi MRT}} \quad [\text{in ms}^{-1}]$$

where M is the molar mass (kg mol^{-1}), $\rho(T)$ is the solid density (kg m^{-3}), R is the perfect molar gas constant ($\text{J mol}^{-1} \text{K}^{-1}$), $\alpha(T)$ is the condensation coefficient, $P_s(T)$ is the saturation vapor pressure at temperature T (K), and P_g is the residual gas pressure (Pa).

[24] Using the density of solid SO_2 (1.928 g cm^{-3} at 77 K) measured by *Post et al.* [1952], this sublimation rate translates into a value of $\alpha(P_s - P_g)$ of $9.0 (\pm 0.25) \times 10^{-9}$ bar. *Honig and Hook* [1960] give a value of P_s of $1.38 (\pm 0.25) \times 10^{-8}$ bar at 120 K (value derived from a thermodynamical curve fit (see section 3.3.2) of their tabulated data: $P_s(\text{bar}) = 2.0 \times 10^6 \sqrt{T} e^{-4200/T}$). After correction of limited recondensation (about 4% of the sublimation rate) from the residual SO_2 pressure in our system this leads to a condensation coefficient $\alpha \approx 0.68 \pm 0.15$. This value is in good agreement with the one found for H_2O ice at similar reduced temperature T/T_m , where T_m is the melting temperature [*Haynes et al.*, 1992]. This provides good confidence in the low temperature extrapolation (< 178 K) of the vapor pressure curve of SO_2 ice given by *Honig and Hook* [1960] (Figure 5). On the other hand, the αP_s curve derived from the sublimation rate equation of *Sandford and Allamandola* [1993] is not consistent with our data. It has a weaker slope than the

P_s curve of *Honig and Hook* [1960] (Figure 5) implying condensation coefficients as low as 0.01 near the melting temperature and values larger than unity below 90 K. The frequently used vapor pressure curve of *Wagman* [1979] gives a value of $P_s(\text{SO}_2)$ at 120 K lower by a factor of 2 compared to *Honig and Hook* [1960], but its simple exponential form ($P_s(\text{bar}) = 1.516 \times 10^8 e^{-4510/T}$) and its too high value at the triple point (+12%) cast some doubt about the accuracy of this equation. We will therefore rely only on the *Honig and Hook* [1960] data in the following.

3.3.2. Cl_2SO_2 Sublimation

[25] A $14.5 \mu\text{m}$ thick sample of solid Cl_2SO_2 was condensed at 120 K and sublimated at 160 K. In this experiment the laser interference fringes were clearly observed during sublimation, thus allowing us to directly measure the sublimation rate from the temporal interferences:

$$\frac{dx}{dt} = \frac{m}{2n\Delta t \nu_{\text{laser}} \sqrt{1 - \frac{\sin^2 \Theta}{n^2}}}$$

where m is the number of interference fringes during the time interval Δt , n is the refractive index at the He-Ne laser wavenumber ν_{laser} , and Θ is its incidence angle. The refractive index of solid Cl_2SO_2 is unknown, as well as its density, but published values exist for liquid Cl_2SO_2 [*Lide*, 1990]. We estimated its density by assuming a density ratio between the solid and liquid phases similar to that of SO_2 ($\pm 15\%$) and derived the associated refractive index from the Lorenz-Lorentz equation. This gave $2.36 \pm 0.35 \text{ g cm}^{-3}$ and 1.675 ± 0.12 , respectively. A sublimation rate of $1.75 (\pm 0.15) \times 10^{-2} \mu\text{m s}^{-1}$ at 160.0 ± 0.2 K was

determined by this technique giving a value of $\alpha(P_s - P_g)$ of $1.03(\pm 0.07) \times 10^{-7}$ bar. The residual Cl₂SO₂ pressure P_g in the cell was about $1.1(\pm 0.3) \times 10^{-8}$ bar during the measurement. If we assume (as found for SO₂) that the condensation coefficient of H₂O ice [Haynes *et al.*, 1992] can be applied to solid Cl₂SO₂ at similar reduced temperature T/T_m ($\alpha \approx 0.60 \pm 0.12$), we derive a saturation vapor pressure of Cl₂SO₂ of $1.85(\pm 0.5) \times 10^{-7}$ bar at 160 ± 0.2 K.

[26] A thermodynamic vapor pressure curve of the form

$$P_s = \frac{A}{\alpha(T)} \sqrt{T} e^{-B/T}$$

has been adjusted between our data point at 160 K and the vapor pressure at the triple point (extrapolated from the vapor pressure curve of liquid Cl₂SO₂; [Lide, 1990]. With $\alpha(T) = 0.60$ the fit gives $A = 1.89 \times 10^9$ bar and $B = 5280$ K for P_s expressed in bar (Figure 5). This law should provide an estimate of the vapor pressure of solid Cl₂SO₂ from the triple point (219.05 K) down to about 100 K with an accuracy better than a factor 2. Most of the uncertainty comes from the assumption on the condensation coefficient $\alpha(T)$ and its temperature dependence. For example, if a linear decrease law $\alpha(T) = 1 - 0.0025 \times T$ (also giving $\alpha(160 \text{ K}) = 0.60$) is used, the extrapolation of P_s at 100 K is 35% higher. On the other hand assuming $\alpha(T) = 1$, as implied for SO₂ if the Wagman [1979] equation is considered, leads to a P_s value 5 times lower.

4. Results and Interpretation

[27] In the following we select the candidate molecules relevant to Io's surface that satisfy the spectral criteria for identification of the 3.920 μm band. We deduce their possible physical states and abundances and assess their probability of occurrence on Io in terms of thermodynamical stability and chemistry.

4.1. Band Identification

[28] An initial literature and database spectral search [Schinanouchi, 2000; J. Crovisier, Molecular Data Base (v 4.1), available at <http://www.usr.obspm.fr/~crovisie/basemole/>, 2001] (mainly gas phase or isolated molecules in matrix) among all possible molecules made of any combination of S, O, H and/or Cl atoms (>50) allowed us to select H₂S (ν_1 and ν_3 modes), H₂S₂ (ν_1 and ν_5), SO₃ ($2\nu_3$), Cl₂SO₂ ($\nu_1 + \nu_6$) and ClSO₂ ($2\nu_1$) as possible candidates for the 3.920 μm band. The fundamental S-H stretching modes of the first two molecules and one first order combination of the S = O stretching modes of the last three have gas phase frequencies that may possibly shift close to the NIMS band position in some condensed state. Simple compounds of S, O, or Cl with Na, K, or Mg (NaO, Na₂O, Na₂S, NaCl, KCl, KO, K₂S, MgO, MgS, ...) have been excluded despite the expected high abundance of some of them [Fegley and Zolotov, 2000] because only very weak third, or larger, order overtones/combinations occur below 4 μm . Only the sulfate compounds (Na₂SO₄, K₂SO₄, MgSO₄, ...) have first order combination modes (SO₄ vibrations) in the NIMS range but their bands are all situated above 4.2 μm and have a wide and complex structure.

[29] Our laboratory measurements first allowed us to eliminate solid SO₃ as its suspected $2\nu_3$ mode, surprisingly occurring at much lower wavelength (around 3.60 μm) than predicted, is far from the NIMS band and because it also displays three stronger bands between 4.03 and 4.10 μm ($\nu_1 + \nu_3$ modes) not observed in NIMS spectra.

4.1.1. Cl₂SO₂

[30] Comparing our laboratory spectra of Cl₂SO₂ with the NIMS band we observe that the $\nu_1 + \nu_6$ band is slightly shifted in the pure solid state (3.902 μm at 110 K) but this shift is reduced to 0.011 μm (about 45% of the NIMS spectral resolution) when Cl₂SO₂ is diluted at the molecular level in solid SO₂ around 110 K (3.909 μm), the mean SO₂ ice temperature on Io [Schmitt *et al.*, 1994, manuscript in preparation, 2003]. A lower temperature can further reduce this shift due to the high thermal sensitivity of this band in the diluted state (see section 3.1). On the other hand, 130 K is probably the maximum compatible temperature.

[31] A simulation of the NIMS spectrum has been performed between 1.5 and 4.7 μm using our radiative transfer model in layered granular surfaces [Douté and Schmitt, 1998] and the optical constants of SO₂ ice at 110 K [Schmitt *et al.*, 1994, manuscript in preparation, 2003] and diluted Cl₂SO₂ at 100 K (see experimental section). High resolution synthetic reflectance spectra generated by the model under the same bidirectional observation conditions than NIMS were then convoluted with the NIMS spectral instrument function (triangular with a FWHM of 0.0243 μm). The Io area corresponding to the spectrum (see Figure 2) was considered to consist of a geographic mosaic of patches of: 1) a Cl₂SO₂:SO₂ solid molecular mixture with uniform composition (both horizontally and with depth), and 2) a spectrally neutral material in the infrared (\sim impure sulfur). The parameters of the model are described in some detail by Douté *et al.* [2001] (see their Table II). We also used the value they derived for the anisotropic scattering parameter ($g = -0.27$). The only additional parameter is the relative molar abundance of Cl₂SO₂ and SO₂.

[32] We obtained the best fit of the spectrum for SO₂ surface proportion ($68 \pm 1\%$) and grain size ($140 \pm 10 \mu\text{m}$) slightly different than the average of the values mapped by Douté *et al.* [2001] for this area of Io ($64 \pm 2\%$, $185 \pm 20 \mu\text{m}$), but they did not use the G2 orbit to derive their map (see their Figures 5 and 6). A quite good overall fit of the position (no residual shift), shape and strength of the 3.920 μm band is obtained at NIMS spectral resolution for a relative Cl₂SO₂/SO₂ molar abundance of $1 \pm 0.2\%$ (Figure 6). This error bar mainly comes from the uncertainty in the absolute calibration of the absorption coefficient extracted for diluted Cl₂SO₂. The derived Cl₂SO₂ abundance is a mean value over the $\sim 100,000 \text{ km}^2$ of the area depicted in Figure 2. Higher values ($\sim 1.5\%$) are obtained for the central pixels of the area where the band is significantly stronger.

[33] Most of the SO₂ bands are well reproduced, although some moderate discrepancies remain in the intensity of the 1.98, 2.125, 3.78, and 4.36 μm bands, possibly due to grain size or temperature distribution (horizontal or vertical) or sulfur contamination [see Douté *et al.*, 2001] or local noise perturbation. However, the main problem is the too strong and wide 3.57 μm feature in our synthetic spectrum corresponding to a blending of the 3.56 μm SO₂ band with the 3.58 μm Cl₂SO₂ band. Comparing this model with

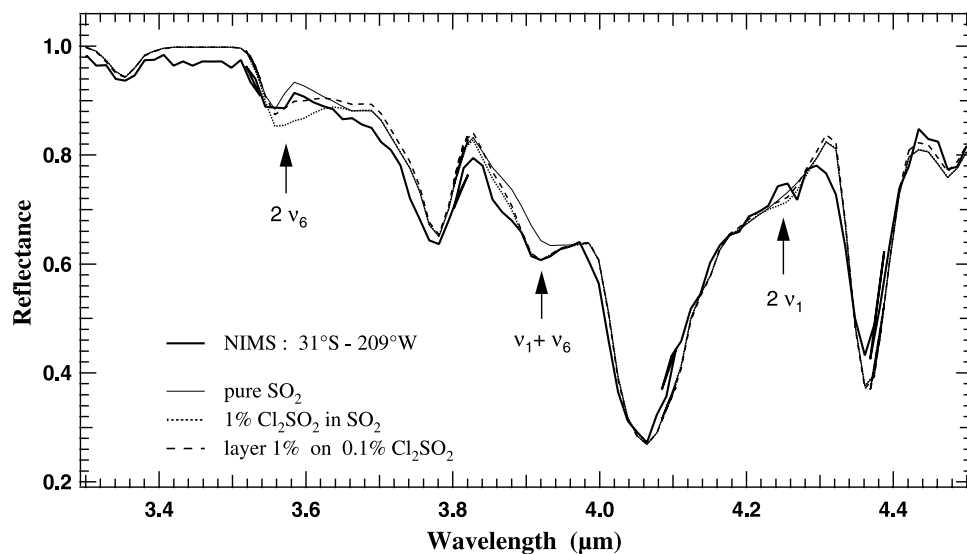


Figure 6. Comparison (3.3–4.5 μm range) between the local NIMS average spectrum (thick line) south of Marduk (31°S–209°W, G2 orbit) and synthetic reflectance spectra convolved to NIMS spectral resolution, involving 1) an optically thick molecular mixture of Cl_2SO_2 and SO_2 (dotted line) with relative molar abundance of 1%:99%; 2) a 1 mm thick layer (for 45% porosity) of the former mixture deposited on a similar mixture but with only 0.1% Cl_2SO_2 (dashed line); and 3) pure SO_2 frost (thin line). In all the above models the SO_2 grain size and surface proportion are 140 μm and 68% respectively. The vertical arrows show the positions of the three bands of diluted Cl_2SO_2 . Note the respective contributions of SO_2 and Cl_2SO_2 .

a simulation without Cl_2SO_2 (with all SO_2 parameters being the same) clearly emphasizes the chlorine molecule contribution to the synthetic spectrum around 3.58, 3.92, and 4.24 μm (Figure 6). The last band is too weak (shoulder 1.5% deep) to be clearly discerned in the wing of the strong 4.07 μm SO_2 band, but the 3.58 μm band with a depth of 7% relative to a pure SO_2 spectrum should emerge from the 3.56 μm SO_2 band in the NIMS spectra. This is clearly not the case.

[34] Several factors may help to reduce the depth of the 3.58 μm band of Cl_2SO_2 without affecting the strength of the 3.920 μm band: First, laboratory measurements showed that the relative peak intensity of the 3.58 and 3.91 μm bands is reduced by a factor of about 8 upon dilution of Cl_2SO_2 in SO_2 ice (from pure to 2% Cl_2SO_2 , Figure 4). At NIMS spectral resolution this decrease is still a factor of 2.3. A further reduction may occur for lower Cl_2SO_2 concentrations, as those found near Marduk (i.e., 1%), but additional experiments need to be performed to assess this possibility. Second, sunlight at 3.58 μm penetrates deeper below the surface, and thus probes more Cl_2SO_2 , than at 3.92 μm due to weaker absorption by SO_2 at the former wavelength. The consequence is an enhancement by about an order of magnitude of the depth of the 3.58 μm band relative to the 3.92 μm band when compared to their respective peak absorption coefficients at NIMS resolution. This enhancement can be reduced if Cl_2SO_2 is concentrated in the top layer of the surface. A simulation of such a stratification of the Cl_2SO_2 abundance (using our layered reflectance model) shows that the 3.58 μm band depth can indeed be reduced to a level compatible with the NIMS data by keeping the Cl_2SO_2 abundance at 1% of in the top layer but decreasing its

value to less than 0.1% in the underlying layer (Figures 6 and 8). The maximum allowable thickness of the top layer ranges between 0.25 and 5 mm for porosities between 10 and 90%, respectively. For thicknesses smaller than about one quarter of these maximum values a Cl_2SO_2 concentration larger than 1% is needed in the top layer to maintain the fit of the 3.92 μm band. In all these simulations the depth of the 4.24 μm shoulder is reduced to less than 1.5% making it virtually unobservable in the wing of the SO_2 band. The average mass of SO_2 contained in this top layer ranges between 50 and 450 g m^{-2} .

[35] The only major remaining misfits in the 2.4–4.5 μm range are on the one hand, the unidentified band around 4.62 μm [Soderblom *et al.*, 1999] and, on the other hand an unidentified broad absorption around 3.15 μm [Carlson *et al.*, 1997], apparently extending up to 3.5 μm and eventually to 3.8 μm if the misfit of the short wavelength wing of the 3.78 μm SO_2 band is due to this same absorption (Figure 8). Preliminary modeling including pure H_2O ice (as a thin top layer or as a granular mixture with SO_2) shows that ice could account only for part of the absorption wing below 3.13 μm , not for the core of the feature. The analysis of these two bands are out of the scope of this paper.

[36] Although the band shift between pure and diluted Cl_2SO_2 is small (8 nm at 110 K), simulations of the Marduk spectrum considering either a granular mixture of pure Cl_2SO_2 and SO_2 grains or a compact slab of pure Cl_2SO_2 on top of pure SO_2 frost display a noticeable short wavelength shift (about one NIMS spectral element, ~ 12 nm) of the 3.92 μm band at NIMS spectral resolution (Figure 7). However, the main arguments in disfavor of the presence of pure Cl_2SO_2 are the intensities of the 3.58 and 4.24 μm bands. In the granular case both bands are too strong ($\sim 10\%$

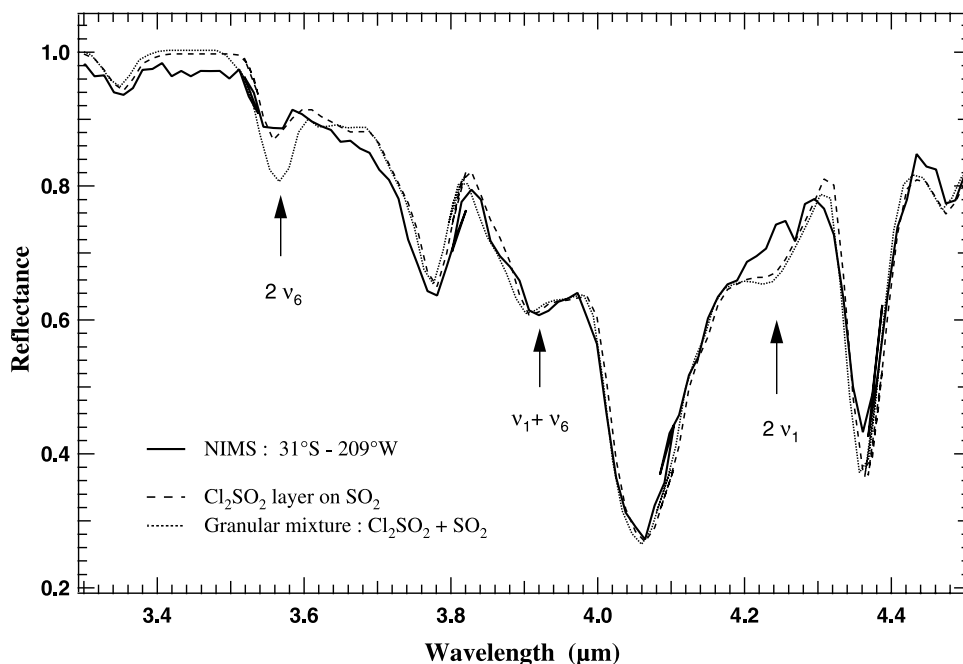


Figure 7. Same as Figure 6 but for 1) a 10 μm thick compact layer of pure Cl_2SO_2 deposited on pure SO_2 frost (dashed line) and 2) a granular mixture of pure Cl_2SO_2 and pure SO_2 grains (dotted line).

and 6% deep, respectively). In the stratified case, with the Cl_2SO_2 layer thickness ($\sim 10 \mu\text{m}$) constrained by the 3.92 μm band depth, the contribution of the 3.58 μm band is sufficiently reduced to allow to fit the 3.57 μm NIMS absorption, but the 4.24 μm band is still too strong ($>4\%$) to be compatible with the observed NIMS spectrum near Marduk (Figure 7).

[37] Let us now consider the three other alternate candidates.

4.1.2. ClSO_2

[38] Unfortunately no laboratory data exist on the combination modes of ClSO_2 in the NIMS range. Only the fundamental modes have been measured in rare gas matrices [Bahou *et al.*, 2000]. We estimated these band positions by analogy with the measured behavior of the similar ν_1 and ν_6 S = O stretching fundamental and combination modes of Cl_2SO_2 (matrix shifts and anharmonicity) (Rodriguez and Schmitt, submitted manuscript, 2003). The frequency of the fundamental ν_1 mode of ClSO_2 diluted in rare gas matrix suggests a position of the first overtone of this mode ($2\nu_1$) around 3.91 μm when diluted in SO_2 , making this molecule an additional good candidate for the 3.92 μm Io band (Figure 8). In the same diluted state the estimated positions for the $\nu_1 + \nu_2$ combination and $2\nu_2$ overtone bands of ClSO_2 are $\sim 4.28 \mu\text{m}$ and $\sim 4.63 \mu\text{m}$, respectively. For pure ClSO_2 the three band positions should differ by no more than 0.01 μm .

[39] The position of the $\nu_1 + \nu_2$ combination band fits quite well with the weak absorption band present at 4.27 μm in the NIMS spectrum of Marduk's "red deposit" (Figure 8), but not in the "SO₂ reference" spectrum (Figure 1). In addition, the estimated $2\nu_2$ overtone wavelength is also in rather good agreement with the $\sim 4.62 \mu\text{m}$ band widely observed on Io by Soderblom *et al.* [1999], and also clearly seen in the Marduk spectrum. This good correlation of band positions for the three main combination bands of ClSO_2

located in the NIMS range elects this molecule to the status of a highly interesting alternative (or competing) candidate. Unfortunately no confirmation of these band positions, no comparison of the band shapes and intensities with Marduk's spectrum, and no modeling of this spectrum can be achieved now to infer the abundance and state of this potential candidate molecule. Laboratory spectra of this poorly known molecule are needed before any confrontation with the "official" candidate Cl_2SO_2 can be performed. However, if a similar band strength is assumed for the first overtone of the asymmetric SO_2 stretching vibration of both molecules ($2\nu_1$ mode for ClSO_2 , $2\nu_6$ mode for Cl_2SO_2) the required abundance of ClSO_2 should be around 5%, more-or-less a factor of a few. Indeed the $2\nu_6$ mode of Cl_2SO_2 is about a factor of five weaker than its $\nu_1 + \nu_6$ mode at 3.91 μm (Figure 4).

4.1.3. H_2S_2

[40] Although the ν_1 and ν_5 stretching modes of gas phase H_2S_2 (3.908 and 3.913 μm ; Schinanouchi, [2000]) fall within less than 0.012 μm of the unidentified band, it is expected from comparison with H_2S that the band position of solid H_2S_2 should be red-shifted by more than 0.05 μm , as it is the case for liquid H_2S_2 (3.986 μm ; [Schinanouchi, 2000]). However, H_2S_2 isolated in solid SO_2 (or S_8) may display a band (containing both modes) close to the gas phase position and thus may still be a potential candidate. Unfortunately no solid phase laboratory spectra of this molecule is available yet to conclude. Using the S-H stretch band strength of H_2S as a typical value for H_2S_2 in our radiative transfer model, we estimate that its molar abundance in solid SO_2 should be of the order of 0.01–0.1% to fit the NIMS band intensity.

4.1.4. H_2S

[41] Diluted H_2S can already be excluded as the absorber of the 3.92 μm band on the basis of our laboratory data (Figures 3 and 4). A modeling shows that 0.08% H_2S

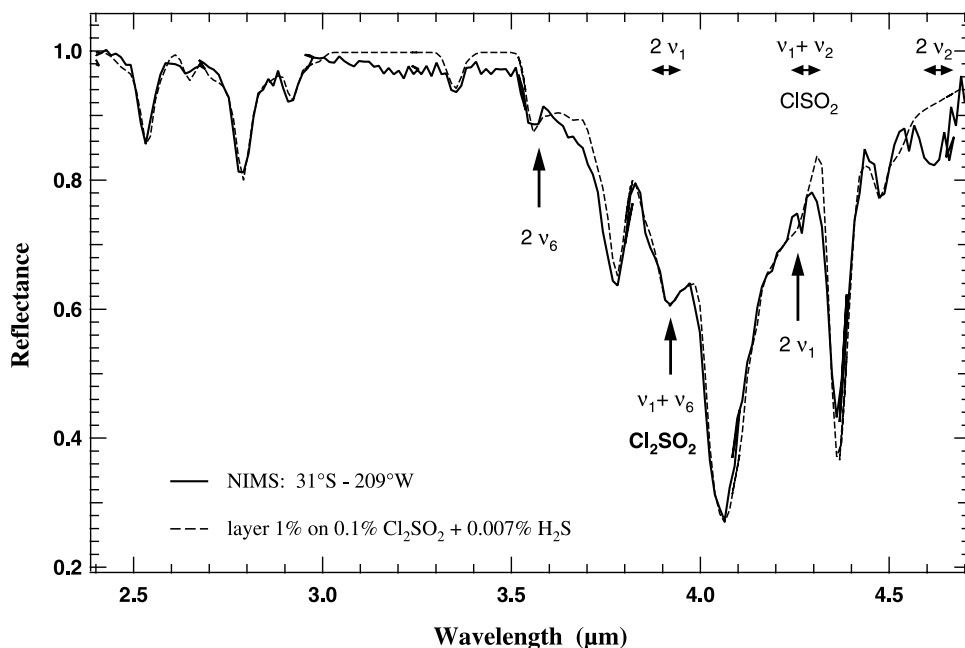


Figure 8. Comparison (2.4–4.7 μm range) of the average NIMS spectrum (thick line) with synthetic spectra involving: a 1 mm thick layer (for 45% porosity) of a molecular mixture of 1% Cl_2SO_2 in SO_2 deposited on 0.1% Cl_2SO_2 diluted in SO_2 with 0.007% H_2S added in both layers (dashed line). SO_2 grain size: 150 μm , surface proportion: 67%. The vertical arrows show the positions of the three bands of diluted Cl_2SO_2 . The horizontal arrows depict probable ranges for the wavelength of the three combination bands of diluted ClSO_2 .

diluted in SO_2 partly fits the 3.92 μm band but displays an additional strong component at 3.85 μm , totally inconsistent with the NIMS spectrum (Figure 9). However, it should be noted that at this low concentration the 3.92 μm component should disappear as it is due to aggregated H_2S molecules (multimers) that only exist at higher concentration (as in our laboratory sample, see section 3.2).

[42] On the other hand, the central band wavelength (3.906–3.910 μm) of the high temperature phases of pure H_2S (above 103.6 K) may barely fit the position of the NIMS band (Figure 4). H_2S should then be segregated from solid SO_2 . It may be in the form of an extremely thin layer condensed on top of solid SO_2 (or sulfur) or less probably dispersed as submicron-sized grains of pure H_2S within the

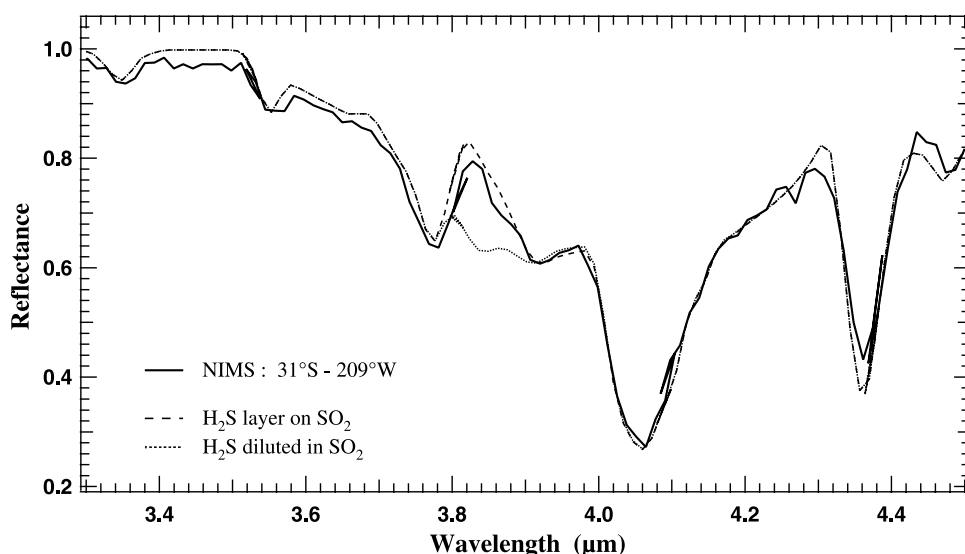


Figure 9. Same as Figure 6 but for 1) a molecular mixture of H_2S and SO_2 (dotted line) with a relative molar abundance of 0.08% and 2) a 0.3 μm thick layer of pure H_2S -II particles (0.1 μm in size) on top of SO_2 ice (dashed line). This last model is equivalent to a compact H_2S layer 0.12 μm thick. The SO_2 grain size is 140 μm .

SO_2 frost. The thickness of the H_2S layer condensed on SO_2 frost (68% of the total area) should be $0.12 \mu\text{m}$ to reproduce the strength and shape of the $3.92 \mu\text{m}$ band, as calculated with the optical constants of pure phase II- H_2S ice at 107 K and considering a thin compact H_2S slab (Figure 9). The weaker H_2S absorptions occurring at 1.952 and $1.995 \mu\text{m}$ have synthetic depths of less than 0.1% and are hidden in the wings of the weak SO_2 band at $1.982 \mu\text{m}$ (~ 1 –1.5% deep). It should be noted that this last band is not seen in the NIMS spectrum of the Marduk area partly due to the noise level ($1-\sigma \sim 0.4\%$).

[43] With our current “geometric optics” radiative transfer model [Douté and Schmitt, 1998] we cannot simulate scattering in an extremely thin layer composed of sub-micron grains. However, Mie calculations show that such a layer composed of spherical H_2S particles less than $0.2 \mu\text{m}$ in diameter behaves like a purely absorbing medium (negligible scattering). We treated this layer independently (neglecting scattering) and coupled it to the reflectance model of the SO_2 substrate. Three monolayers of $0.1 \mu\text{m}$ particles (or correspondingly more layers for smaller particles) are required to fit the $3.92 \mu\text{m}$ NIMS band depth implying a layer thickness in the range 0.3 – $4 \mu\text{m}$ for 30 to 95% porosity. The local thickness of this layer may be increased if we consider that only a fraction of the area covered by SO_2 ice has condensed H_2S on top. However, for thicknesses larger than $4 \mu\text{m}$ (for the minimum 30% porosity for a sphere layer) and fractional area lower than 8% the $3.92 \mu\text{m}$ band starts to saturate, debasing the fit.

[44] It should be noted that crystalline phase III of solid H_2S is excluded because it should display a double band structure peaking around 3.92 and $3.955 \mu\text{m}$ (see Figure 4) at NIMS spectral resolution, the second one being clearly incompatible with the observations. This sets a minimum temperature of 103.6 K for condensed H_2S on Io.

[45] Finally, though diluted H_2S is excluded as the main source of the $3.92 \mu\text{m}$ absorption, adding a minor amount of H_2S ($\sim 7 \times 10^{-5}$) in our stratified Cl_2SO_2 : SO_2 models slightly improves the fit in the short wavelength wing of this band (Figure 8). Although not a tangible proof of the occurrence of diluted H_2S , it sets an upper limit of $\sim 10^{-4}$ for its abundance in solid SO_2 .

4.1.5. Identification Summary

[46] To sum up, direct comparison between laboratory spectra and the average Marduk NIMS spectrum, coupled with radiative transfer modeling, allows us to propose as the surface material producing the $3.92 \mu\text{m}$ absorption either (1) a (sub)micron thin layer of pure solid H_2S (phase II), either compact or made up of submicron particles, condensed at $T \geq 103.6 \text{ K}$ on top of the SO_2 ice, or (2) a millimeter thick layer of 1% Cl_2SO_2 mixed at the molecular level within solid SO_2 covering a similar mixture but strongly depleted in Cl_2SO_2 ($< 0.1\%$). There is no severe constraint on temperature, but it is probably lower than 130 K .

[47] Spectral constraints on the $3.92 \mu\text{m}$ band alone, are not able to unambiguously distinguish between these two possible identifications. Unfortunately, both molecules do not possess other bands strong enough and far-off the SO_2 bands to clearly appear in the NIMS data and thus to firmly confirm one of these candidates. H_2S has a few additional bands around $1.98 \mu\text{m}$ but they are too weak to be observable in the NIMS Marduk spectrum. For diluted

Cl_2SO_2 we found that only a limited additional physical constraint (stratification) is necessary to hide its two weaker bands (at 3.58 and $4.25 \mu\text{m}$) within the SO_2 absorptions.

[48] Finally, in the absence of relevant laboratory spectra, theoretical considerations also led us to consider diluted ClSO_2 (about 2–15% in solid SO_2) and diluted H_2S_2 (0.01–0.1%) as two additional potential candidates. ClSO_2 is particularly attractive as it may fit, or contribute, to two other bands at $4.27 \mu\text{m}$ (weak) and $4.62 \mu\text{m}$ (strong and broad).

[49] The problem is now to find additional arguments in terms of chemistry and volatility that may help to discern between these four possible candidate molecules and to estimate their probability of occurrence in their respective physical states under Ionian conditions.

4.2. Chemistry and Volatility

[50] The molecules condensed at the surface of Io are expected to come mostly from volcanic eruptions or lava degassing [Zolotov and Fegley, 1998a, 1998b; Fegley and Zolotov, 2000] followed by photochemistry in the transient atmosphere [Summer and Strobel, 1996; Wong and Johnson, 1996a; Moses et al., 2002a, 2002b] and possible evolution by energetic particle bombardment at the surface [Moore, 1984; Wong and Johnson, 1996b; Johnson, 1997]. SO_2 , H_2S , and Cl_2SO_2 have been included in the equilibrium chemical model of the volcanic gases [Fegley and Zolotov, 2000] and in the photochemical model of Moses et al. [2002a, 2002b]. ClSO_2 and H_2S_2 were not taken into account in the volcanic model. The results for H_2S and H_2S_2 were not discussed in the Moses et al. [2002a, 2002b] papers due to the very low assumed elemental H abundance. The possible chemical reactions of the atmospheric gases with the surface materials and upon condensation have not yet been considered in models, but the possibility of heterogeneous reactions has been discussed by Moses et al. [2002a, 2002b].

[51] Besides the chemical considerations, the volatility of the candidate materials has to be taken into account in the elaboration of volcanic gas condensation scenarios able to produce the inferred physical states and molecular abundances at the surface. Extrapolations at low temperatures of the vapor pressure curves exist for solid SO_2 and H_2S [Honig and Hook, 1960] but are restricted to the liquid phase above 225 K for H_2S_2 and Cl_2SO_2 . We derived this curve down to $\sim 100 \text{ K}$ for solid Cl_2SO_2 (see experimental part and Figure 5).

[52] In the following we will first compare, for each candidate molecule, the abundances we deduced in the solid phase with those expected for the volcanic gases from existing chemical models. Then we consider the volatility of these molecules to propose condensation scenarios and to assess the condensate stability at Io's surface under plausible temperature and pressure conditions. Finally, scenarios considering possible heterogeneous reactions are investigated.

4.2.1. Cl_2SO_2

[53] Within the range of volcanic conditions studied by Fegley and Zolotov [2000] their chemical model falls far short of producing enough Cl_2SO_2 molecules to account for the intensity of the $3.92 \mu\text{m}$ band. However, preliminary calculations by M. Zolotov (Washington University, personal

communication, 2000) show that the abundance of Cl_2SO_2 may be increased by 2 to 4 orders of magnitude and reach a mole fraction relative to SO_2 of 5×10^{-7} to 5×10^{-5} under particular physical conditions in the vent ($T = 1000$ K, $P = 1$ to 100 bar) but with O and Cl atomic compositions ($\text{O/S} = 2$, $\text{Cl/S} = 0.10 - 0.20$) exceeding the upper limits of Io's torus. If directly applied to surface condensates, these Cl_2SO_2 abundances are still too low by more than two orders of magnitude to account for the NIMS band intensity, but possible specific (though extreme) local vent conditions and chemical composition at Marduk may further increase the volcanic production of Cl_2SO_2 . In particular, larger O/S and Cl/S atomic ratios and lower magma temperatures may favor Cl_2SO_2 over the other, generally more abundant, nonoxidized Cl_xS_y chlorine compounds. On the other hand, atmospheric photochemistry seems unable to help significantly in that direction (*J. Moses*, Lunar and Planetary Institute, personal communication, 2001) because three-body reactions, inefficient in the low density Io atmosphere, are necessary to form ClSO_2 , the essential precursor of Cl_2SO_2 [*Moses et al.*, 2002b].

[54] It is interesting to note at this point that, even if we directly apply the enhanced chlorine atmospheric abundances obtained by M. Zolotov (under the above volcanic conditions) to surface composition and combine them with molecular band strengths, the $3.91 \mu\text{m}$ band of diluted Cl_2SO_2 may be already the "strongest" near-IR band of all 13 chlorine molecules included in the volcanic model. However, its depth would be only 0.03% for 3×10^{-5} Cl_2SO_2 abundance! Although Cl_2SO is generally slightly more abundant in the volcanic models, we found experimentally that its only near infrared band near $4.15 \mu\text{m}$ ($2\nu_1$) is inactivated when diluted in solid SO_2 (Rodriguez and Schmitt, submitted manuscript, 2003). ClO and Cl_2O have much too low abundances to have their second order overtone/combination bands observable in the NIMS range. Atomic Cl and the Cl_2 molecule are infrared-inactive. Even the most abundant chlorine-bearing molecules, NaCl , KCl , ClS , ClS_2 , Cl_2S , and Cl_2S_2 , have their fundamental bands at too low frequencies ($>14 \mu\text{m}$) to have observable overtone/combination modes (Rodriguez and Schmitt, submitted manuscript, 2003). Finally only the very strong bands of HCl around $3.5-3.6 \mu\text{m}$ may show up if its abundance exceeds about 10^{-5} , that is for H/S atomic ratios larger than 10^{-4} according to *Fegley and Zolotov* [2000]. But its very high volatility (2×10^5 times that of SO_2 at 110 K [*Honig and Hook*, 1960]) does not favor its condensation at Io surface temperatures.

[55] However, extreme volcanic conditions producing high Cl_2SO_2 gas abundances are not requisite to reach 1% in the frost. Indeed, thermodynamical equilibrium between the atmospheric and condensate compositions should trigger a chemical differentiation that strongly enhances the concentration of the less volatile molecules, such as Cl_2SO_2 , in solid SO_2 .

4.2.1.1. Condensation Scenario

[56] From the extrapolation of the vapor pressure curves of solid SO_2 [*Honig and Hook*, 1960] and Cl_2SO_2 (Figure 5) we determine a nominal saturation pressure ratio $P_s(\text{SO}_2)/P_s(\text{Cl}_2\text{SO}_2)$ of about 12,000 at 110 K, but possible values may range between 6,000 and 30,000 depending on the assumed value for the condensation coefficient of

Cl_2SO_2 (see experimental part). The upper limit of the ratio results from the assumption of unity condensation coefficient.

[57] If a SO_2 -rich ($\sim 65\%$) volcanic gas containing Cl_2SO_2 condenses rapidly on cold surfaces surrounding the vent (i.e., when the SO_2 gas pressure over the surface is much larger than its saturation pressure at the surface temperature) then Cl_2SO_2 should be dynamically trapped in SO_2 ice with a similar mole fraction than in the gas. However, if this condensation occurs in conditions close to thermodynamical equilibrium (i.e., with a small pressure ratio $P(\text{SO}_2)/P_s(\text{SO}_2, T_{\text{surf}})$), a Cl_2SO_2 mole fraction of only 5×10^{-7} is necessary to obtain a concentration of 10^{-2} in solid SO_2 at 110 K, assuming ideal solid solution (i.e., following Raoult partial pressure law). The $\text{Cl}_2\text{SO}_2:\text{SO}_2$ mixture probably do not form an ideal solid solution, therefore the Cl_2SO_2 equilibrium partial pressure may need to be larger than 5×10^{-7} by an unknown factor (the activity coefficient). The equilibrium concentration in the solid is also temperature dependent (decreasing with increasing surface temperature, as $P_s(\text{SO}_2)/P_s(\text{Cl}_2\text{SO}_2)$, see Figure 5) but SO_2 condensation should not occur above 140 K over large area if the plume pressure drops below 10^{-6} bar a few kilometers away from the vent [*Zhang et al.*, 2003]. At 140 K, a Cl_2SO_2 mole fraction of 4×10^{-6} is then needed to equilibrate 10^{-2} in solid SO_2 . On the other hand, condensation of almost pure solid Cl_2SO_2 requires a Cl_2SO_2 mole fraction in the gas larger than 10^{-3} , a highly improbable value.

[58] However, for this scenario to work most of the erupted SO_2 (99.99%) should not condense in the reddish area to maintain the 1% Cl_2SO_2 abundance observed in the top frost layer. It can flow away but no sign of massive condensation outside the Marduk deposits is observed. If all this SO_2 ($\sim 10^{14}$ kg) is injected in the atmosphere, the implied global Io resurfacing rate is thousands of times the Pele rate [*Spencer et al.*, 1997]. Consequently this gas-solid differentiation scenario is difficult to support.

4.2.1.2. Heterogeneous Formation Scenario

[59] Besides volcanic and atmospheric chemistries and condensation scenarios other chemical pathways may be considered to explain the high Cl_2SO_2 abundance at the surface.

[60] Starting from our initial reports on the possible identification of large amounts of Cl_2SO_2 near Marduk [*Schmitt and Rodriguez*, 2000, 2001] and from subsequent discussions on the possible chemical pathways toward Cl_2SO_2 , an alternative possibility to form this molecule directly at the surface by heterogeneous reaction has been pinpointed by *Moses et al.* [2002b]. Laboratory investigations of the reactions occurring during UV irradiation (308 nm) of Cl_2 and SO_2 mixed in rare gas matrices [*Bahou et al.*, 2000] show that successive reactions of Cl atoms (formed by photo-dissociation of Cl_2) with SO_2 first form ClSO_2 , then Cl_2SO_2 .

[61] On Io a high atomic Cl abundance is directly produced in the volcanic magma when the elemental ratio $\text{Cl}/(\text{Na} + \text{K})$ exceeds unity [*Fegley and Zolotov*, 2000]. Most of the excess Cl is in atomic form. Its abundance is then slightly increased in the atmosphere (by about 0.2% for a typical 20 min plume flight time) by photolysis of NaCl and KCl [*Moses et al.*, 2002b]. On the other hand, condensed SO_2 is ubiquitous at

the surface of Io, even at short distances from active vents [Douté *et al.*, 2001, 2002], and also possibly forms in some volcanic plumes [Spencer *et al.*, 1997; Cataldo and Wilson, 1999]. It then appears that two necessary conditions for heterogeneous reaction of atmospheric Cl with condensed SO₂ are met. However, several major pieces of information are missing to quantify the production efficiency of Cl₂SO₂ in the different scenarios that can be proposed.

[62] First, the single laboratory study available today [Bahou *et al.*, 2000] is only qualitative and thus did not allow us to infer the efficiency of the process, especially at Io's surface or plume conditions. In particular when Cl directly reacts on a solid SO₂ surface, the reaction may follow a different chemical pathway to Cl₂SO₂ than in rare gas matrices. It should be also noted that Bahou *et al.* [2000] found that a small energy barrier should be overcome to form Cl₂SO₂ from ClSO₂. Thermal energy at Io's surface temperature might be sufficient to trigger this reaction. This barrier might also not exist for direct reaction with solid SO₂. New experiments are urgently needed to solve these issues.

[63] The second major unknown is the chemical composition of the gases released during the eruption of Marduk. This volcano may be quite atypical on Io owing to its particular fan-shaped reddish deposit that is suspected to exhibit high pressure style eruption [McEwen *et al.*, 1998]. S₃ and S₄ radicals are suspected to produce this reddish color [Spencer *et al.*, 2000; McEwen *et al.*, 1998; and references therein], but as we will show later, Cl₂S might be an alternative, or competing, source for this coloration. However, the discrimination and quantification of these molecules are not yet possible due to a lack of laboratory data, and no other compositional information is available to constrain the chlorine content in the plume and near the surface.

[64] Another key question is: do the heterogeneous reactions leading to Cl₂SO₂ occur on SO₂ particles condensing in the volcanic plume, or directly at the surface on condensing SO₂ frost or, as suggested by Moses *et al.* [2002b], on adsorbed SO₂? Indeed, it is not yet completely clear what is the effective process of SO₂ "frost" formation in the annular or irregularly shaped "deposits" around volcanos. Models of SO₂ condensation in the plume [Cataldo and Wilson, 1999] as well as direct (ballistic) SO₂ deposition on the surface [Glaze and Baloga, 2000] have been recently proposed.

[65] The situation certainly depends on the volcano and of the type of eruption. Using the plume particle sizes and masses derived by Spencer *et al.* [1997] for Pele and Loki we can compare the condensation time constants of SO₂ and Cl on the plume particles with the typical flight time of the plume and infer if significant SO₂ condensation and Cl reaction may occur on the plume particles.

[66] Assuming the SO₂ gas is greatly supersaturated in the plumes and that the particles are smaller than the mean free path of the gas (true for Io's plumes), the condensation time constant τ_c (derived from gas kinetic laws) of the gas on particles of radius r_p and number density n_p is

$$\tau_c = \frac{1}{\langle c \rangle \alpha n_p \pi r_p^2} \quad \text{with} \quad \langle c \rangle = \sqrt{\frac{8RT}{\pi M}}$$

where $\langle c \rangle$ is the mean speed of the condensible molecules and M is their molar mass.

[67] In the case of Pele we consider the two extreme particle radii and associated total masses of the plume (2.8×10^9 g for 0.05 μm particles, 1.15×10^9 g for 0.08 μm) derived by Spencer *et al.* [1997] from their modeling of the wavelength dependent optical depth of the plume. Assuming an homogeneous hemispheric plume with radius 420 km we derive particle number densities of 1.7×10^7 partic. m^{-3} (0.05 μm) and 1.7×10^6 partic. m^{-3} (0.08 μm). With these parameters we obtain time constants of 15 h and 60 h for SO₂ (with $\alpha = 0.68$) and Cl (with assumed $\alpha = 0.5$) for the 0.05 μm and 0.08 μm particle cases, respectively. These values are much larger than the typical plume time of flight (~ 20 min). However, for Loki (with 200 km plume radius) the figure dramatically changes. For the assumed 0.01 μm particle radius and the plume mass of 9.3×10^{10} g calculated by Spencer *et al.* [1997] we obtain a particle number density of 6.6×10^{11} partic. m^{-3} and condensation time constants of only 30 s for SO₂ and Cl. This value is almost two orders of magnitude lower than the time of flight, thus strongly favoring SO₂ condensation and possible reactions of Cl on the plume particles. The heterogeneous reactions of Cl atoms with SO₂ condensing on very fine particles (~ 0.1 – 0.01 μm) are also favored by the large surface area available in the volcanic plume. For Loki the total area of the particles is 10–100 times larger than the plume deposit area.

[68] There is not yet published plume optical depth analysis at Marduk, but a "visible plume" (measured at 0.42 μm) is quoted in the SSI images during the G8, E11, and possibly E6, C9 and C10 Galileo orbits by McEwen *et al.* [1998]. As Marduk has a "prometeus-type plume" (larger optical depth than Pele) and is suspected to have "overpressured eruptions", we can suspect rather favorable pressure and particle density conditions for SO₂ to condense efficiently in the plume and for atomic Cl to meet SO₂ and react with it on the particles. Given the very short expected condensation time scale the full condensation-reaction process may well mostly occur in the very first minute(s) of the plume flight. During that time continuous SO₂ condensation in the plume allows to progressively incorporate in the particles the Cl₂SO₂ molecules freshly formed at their surfaces. This also renews the SO₂ surface for further reactions. Given the much lower evaporation rate of Cl₂SO₂ compared to SO₂, the trapping process should be very efficient. Even if the particle composition constantly equilibrates with the gas phase during all this process, the loss of Cl₂SO₂ to the gas should be negligible as a gaseous mole fraction of only $\sim 10^{-6}$ Cl₂SO₂ is needed to stabilize 1% in solid SO₂. This scenario is compatible with the deduced physical state of Cl₂SO₂, i.e., diluted at the molecular level within the SO₂ grains.

[69] In this process a minimum Cl/SO₂ ratio of 2% is needed to produce 1% Cl₂SO₂ in solid SO₂ if we assume 1) similar sticking coefficients for Cl and SO₂ on a SO₂ particle, 2) complete conversion of adsorbed Cl to Cl₂SO₂, 3) no chemical or thermal desorption of Cl, ClSO₂, Cl₂SO₂ or SO₂, and 4) all the available SO₂ condenses on the particles. In fact the sticking coefficient of Cl on SO₂ ice is probably lower than the condensation coefficient of SO₂, but on the other hand the thermal desorption rate of SO₂

may be a significant fraction of its condensation rate, depending on particle temperature and plume conditions. Part of the Cl atoms may also desorb before reaction or react with other molecules or radicals condensed with SO_2 and a fraction may be locked in ClSO_2 isolated in solid SO_2 before being able to react with another Cl atom. Finally a significant part of the volcanic SO_2 may not condense on the particles and escape from the plume thus contributing to the background Io atmosphere. Favorable conditions for effective heterogeneous formation of Cl_2SO_2 on plume particles are then met only for Cl-rich volcanic eruptions (i.e., $[\text{Cl} - (\text{Na} + \text{K})]/\text{S} > 0.015$) and when the particle density in the plume is high enough to allow efficient SO_2 condensation and Cl sticking. For a global efficiency of the Cl_2SO_2 formation process of about 50%, and for $(\text{Na} + \text{K})/\text{S} = 0.02$ the formation of 1% Cl_2SO_2 relative to SO_2 may require a Cl/S ratio of 0.05.

[70] If SO_2 condensation did not occur in the plume, fresh SO_2 frost should directly develop at the surface and the chlorine atoms should then react with the SO_2 molecules condensing on the frost crystal surfaces (i.e., with the top molecular layer, considered as “adsorbed SO_2 ” by *Moses et al.* [2002b]) in a way similar to that on plume particles. So the formation of Cl_2SO_2 should only occur where and when the SO_2 molecules condense. On the other hand it is difficult to imagine a scenario in which Cl efficiently reacts with SO_2 grains previously condensed or deposited at the surface. Indeed, the poorly volatile Cl_2SO_2 molecules accumulating as a monolayer at the surface of the grains (typically larger than 10–50 μm [*Douté et al.*, 2001]) probably hinder further reaction between Cl and SO_2 .

[71] We were also not able to imagine a simple scenario, consistent with our observations, in which Cl reacts with SO_2 adsorbed in “warm” area, as proposed by *Moses et al.* [2002b]. Indeed, only part of the volcanic SO_2 will adsorb in these warm area, but most of the available Cl should adsorb and react with this SO_2 and form Cl_2SO_2 , otherwise extreme Cl/S ratios are needed. This weakly volatile molecule should then efficiently desorb to go back and mix in the ballistic plume and then cocondense with the bulk of SO_2 to form the observed millimeter thick intimately mixed $\text{Cl}_2\text{SO}_2:\text{SO}_2$ solid deposit. We rather think that the Cl_2SO_2 molecules possibly formed in this way will be predominantly segregated in the “warm” area where they formed.

[72] Once deposited or formed at the surface, the frost composition should be stable as the millimeter thick Cl_2SO_2 -rich layer contains more than 10^7 times the Cl_2SO_2 amount required to maintain its equilibrium partial pressure in the whole atmospheric column above the deposits.

[73] At the surface Cl_2SO_2 is destroyed by UV radiation with a time constant of about 3 years ($\lambda < 360 \text{ nm}$, $J \approx 10^{-8} \text{ s}^{-1}$ [*Moses et al.*, 2002b]). The SO_2 ice matrix adds some UV protection as a thickness of only a tenth of a millimeter completely absorbs all solar radiations below 320 nm and a decreasing fraction of the wavelengths up to 370 nm [see, e.g., *Nash et al.*, 1980]. Adding a small amount of sulfur molecules (0.5%–3% S_8) in SO_2 strongly decreases the UV penetration depth below 400 nm [see *Douté et al.*, 2001]. In this case an almost complete shielding of Cl_2SO_2 from UV photolysis is achieved.

[74] In addition any Cl atom formed by photolysis of Cl_2SO_2 will react immediately with the surrounding SO_2

matrix molecules to form ClSO_2 , the precursor of Cl_2SO_2 . This may explain why Cl_2SO_2 was still present in similar amount in the Marduk deposits at the time of the E14 encounter (March 1998), 1.5 years after the G2 observation. The Cl_2SO_2 molecules will be exposed to UV radiation only when the SO_2 matrix will slowly sublimate through the day-night cycles, i.e., after the plume supply will stop. A progressive segregation of Cl_2SO_2 (as a pure solid or mixed with sulfur) from SO_2 may then occur, depending on the local conditions.

[75] The thickness of the Cl_2SO_2 -rich layer (0.2–0.5 mm with unit compacity) may reflect the amount of gas condensed during the last eruption(s) of Marduk (post Voyager): of the order of 5×10^9 – $5 \times 10^{10} \text{ kg}$ of SO_2 frost over the whole reddish area. Marduk was probably active at the time of the G2 observations (September 1996) as plumes were still visible above the volcano during at least the next 8 months (orbits E6, G8 [see *McEwen et al.*, 1998]).

[76] The lower concentration deduced for the underlying layer may be due either to different volcanic conditions (lower $[\text{Cl} - (\text{Na} + \text{K})]/\text{S}$ abundance ratio, for example) during the previous eruption or to the burial of Cl_2SO_2 below a layer of “pure” SO_2 ice before being overlaid by the frost coming from the last eruption. Indeed, the day-night sublimation-condensation cycle may segregate the less volatile Cl_2SO_2 molecules and accumulate a couple of millimeters of pure SO_2 frost on top, enough to hide the overlaid Cl_2SO_2 from the solar infrared photons. Only Cl_2SO_2 deposited in the top layers by the last eruption is then being probed. On the other hand, as demonstrated before, the complete depletion by UV photo-destruction of Cl_2SO_2 in the SO_2 layer takes more than a decade.

4.2.2. ClSO_2

[77] The heterogeneous formation mechanism of Cl_2SO_2 observed by *Bahou et al.* [2000] requires the intermediate formation of ClSO_2 , as in the gas phase. Although only a minor atmospheric product on Io [*Moses et al.*, 2002b] this molecule may be formed on SO_2 ice and trapped in appreciable quantity, especially if its reaction with another Cl atom and subsequent conversion to Cl_2SO_2 is hindered by some energy barrier, as suggested by *Bahou et al.* [2000]. A high condensation rate of volcanic SO_2 on plume particles or on surface grains, eventually coupled with a low atomic Cl abundance, may also isolate this first reaction product into solid SO_2 before another Cl atom may react with it. On the other hand ClSO_2 is a quite unstable molecule and easily decomposes under reaction with most atoms and molecules [see *Moses et al.*, 2002b]. Some condition dependent partition or steady-state balance between production and destruction of these two molecules may occur. Both molecules are then likely to be simultaneously present but in a unknown ratio. Preliminary results from recent experiments on the heterogeneous formation of Cl_2SO_2 seem to show that, contrary to the results of *Bahou et al.* [2000], ClSO_2 may be only a minor product (L. Schriver and A. Schriver, Université P. & M. Curie, personal communication, 2002).

[78] We should also note here that only half the amount of Cl required to form Cl_2SO_2 is necessary for the formation of ClSO_2 . But on the other hand, a larger amount (2–15% in SO_2) may be required to fit the 3.92 μm band strength if the intrinsic strength of the $2\nu_1$ ClSO_2 band is effectively

weaker (see section 4.1.2). This may further increase the constraint on the abundance of atomic Cl (in excess of Na + K) in the atmosphere of Io if this molecule is effectively the main absorber at 3.92 μm in the Marduk spectrum.

4.2.3. H₂S

[79] The H₂S gas abundance may be inferred from the number of H₂S molecules segregated in the candidate submicron top layer only if the differentiation process and scenario that led to it are assumed. The thermodynamical properties of solid H₂S and SO₂ should be taken into account to assess if such a differentiation is realistic on Io.

[80] The very high volatility of H₂S ice (vapor pressure 10⁴ times that of SO₂ around 110 K [Honig and Hook, 1960]) (Figure 5) makes it very unstable even at temperatures as low as 103.6 K, the minimum temperature of occurrence of the crystalline phase II of solid H₂S compatible with the observation. At this temperature a partial pressure of 1.5×10^{-6} bar is necessary to stabilize a layer of pure solid H₂S. Even if we consider a H₂S mole fraction in the gas as large as 10⁻⁴, a total pressure above 0.01 bar is then needed. Such a high pressure on Io may possibly occur locally near erupting vents but then SO₂ should condense very rapidly and dynamically trap H₂S at the low gas concentration. If condensation occurs under thermodynamical equilibrium with the above gas composition, then the concentration of H₂S in solid SO₂ will be about 10⁻⁷–10⁻⁸ depending on condensation temperature. Both scenarios lead to diluted H₂S and thus are unable to fit the NIMS 3.92 μm band position and shape. Diluted H₂S, if present, may however marginally contribute to the NIMS spectrum (in the wing around 3.85 μm) for concentrations ranging from a few 10⁻⁵ to a maximum of 10⁻⁴ (Figures 8 and 9). For surface temperatures around 110 K these concentrations imply local H₂S equilibrium pressures in the range 5×10^{-11} – 1×10^{-9} bar, i.e., just above the upper limit found for the global H₂S background atmosphere [Lellouch *et al.*, 1990].

[81] As the gas expands away from the vent source the pressure drops and SO₂ condenses on progressively colder plume particles or surfaces. If this occurs sufficiently slowly (i.e., close to equilibrium) the SO₂ ice should trap most of the less volatile plume molecules but only a minor fraction of H₂S. The H₂S mole fraction in the gas will progressively increase due to preferential SO₂ condensation. At some point, when most of the SO₂ will have condensed, the remaining gas may be dominated by the more volatile H₂S, with possibly some HCl and Cl₂. Phase II H₂S-rich ice may then condense on cold area if its partial pressure has not dropped below 1.5×10^{-6} bar. Considering a maximum gas pressure at the vent output of 10 bar and a minimum gas expansion factor of 10³ at the condensation zone [Zhang *et al.*, 2003], a minimum initial H₂S abundance in the gas of 10⁻⁴ is necessary to maintain such a high partial pressure as far as 100 km from the vent (the typical extent of the material producing the 3.92 μm band). However, if the H₂S pressure drops below 10⁻⁶ bar the time to completely sublimate a micron-thick layer of solid H₂S will be less than one minute at 104 K. So any thin deposit of solid H₂S-II should be very unstable and ephemeral. This is in complete contradiction with the persistence of the 3.92 μm band on Io over at least 1.5 years. Sublimation time scales

of that order imply temperatures as low as 70 K, and thus solid phase III H₂S.

[82] Now, considering the chemical aspects of H₂S, the volcanic model may produce enough of this molecule to account for the band strength. However, 10 times more H₂O is formed with H₂S (with O/S = 1), independently of the hydrogen abundance [Fegley and Zolotov, 2000]. This ratio is certainly higher for larger O/S atomic ratios. There is no sign in the NIMS spectra of the presence of the strong band of diluted H₂O around 2.7 μm (Figure 1) but H₂O is probably segregated from the SO₂ frost owing to their very different volatilities. If we consider that pure H₂O ice contributes to the wing of the unidentified 3.15 μm NIMS absorption (Figure 8), an upper limit of 0.04 is deduced for the H₂O/H₂S abundance ratio. This value is smaller by more than 2 orders of magnitude than the predicted abundance ratio but specific chemical conditions (O/S \ll 1, ...) may possibly release the H₂O constraint on the local H₂S abundances. The expected strong differential H₂O and H₂S segregation from SO₂ frost may also have hidden H₂O (below a few millimeters of SO₂ frost, for example) in area where H₂S condensed on top of the frost. So the nonobservation of H₂O does not allow us to strictly exclude the presence of an observable amount of H₂S.

[83] In addition to the water molecule, HCl and NaOH are produced with abundances around 10⁻⁴ when H₂S is formed in the 10⁻⁴–10⁻² range in the nominal volcanic conditions considered by Fegley and Zolotov [2000]. The fundamental HCl band falls within the 3.56 μm SO₂ band but should be detectable above 10⁻⁵ mole fraction. However, owing to its 30 times higher volatility than H₂S, its nonobservation on the surface cannot strongly constrain the H₂S abundance. On the other hand NaOH, with a very low volatility, sets similar constraints than H₂O.

[84] A high H₂S abundance ($>10^{-4}$) also implies a volcanic H/S atomic ratio larger than 10⁻³ [Fegley and Zolotov, 2000]. With the upper limit of H atom number density of $1.1 \times 10^4 \text{ cm}^{-3}$ above the surface and the average SO₂ pressure of 0.2–0.35 nbar implied by the Lyman alpha HST observations [Strobel and Wolven, 2001], a H/S atomic ratio of less than 10⁻⁶ is deduced near the surface. This is perhaps the most severe constraint on H/S, but on the one hand it is a global value that takes into account only atomic H, not the hydrogenated molecules like H₂S, and on the other hand there are now converging evidences that the Io plasma torus, and not the surface, may supply most of the atmospheric H [Roesler *et al.*, 1999; Strobel and Wolven, 2001]. We should also note that H₂S⁺ has been inferred from a peak observed by Galileo in a single spectrum of ion cyclotron waves at a few Io radii from the surface [Russell and Kivelson, 2001]. However, this identification is only tentative and we suspect a possible contribution from ³⁴S⁺ (a smaller unidentified peak is also observed at the position of ³³S⁺).

[85] To sum up, the chemical constraints did not favor the constant supply of the high volcanic H₂S abundance ($>10^{-4}$) required to eventually stabilize over months, or years, an ultra-thin H₂S frost layer covering the Marduk deposits.

4.2.4. H₂S₂

[86] Although H₂S₂ is not currently included in the volcanic model of Fegley and Zolotov [2000], it is probably

formed with an abundance much lower than HS and should follow a similar trend as a function of the H/S ratio (same reduction state). The vapor pressure of H_2S_2 is unknown in the solid state but from thermodynamical extrapolation of the liquid curve [Lide, 1990] we derive a saturation pressure 10^4 – 10^5 times smaller than SO_2 at 110 K. Consequently the concentration of H_2S_2 diluted in SO_2 (10^{-4} – 10^{-3}) estimated to produce the NIMS absorption band needs an equilibrium abundance of about 10^{-9} – 10^{-7} in the gas. However, as for Cl_2SO_2 , such a large differentiation creates the unsolvable problem of the destiny of the superfluous SO_2 . If no, or only a limited, differentiation occurs (i.e., H_2S_2 is mostly dynamically trapped by SO_2 condensing on plume particles or at the surface) a H/S atomic ratio larger than 10^{-2} is implied even if we assume that H_2S_2 is formed in the volcanic vent at an abundance just a few times lower than HS [Fegley and Zolotov, 2000]. Such an unexpectedly high H/S ratio is clearly in conflict with the much smaller global atmospheric value obtained by Strobel and Wolven [2001]. In addition, H_2S and H_2O should form in exceedingly large amounts ($>10^{-3}$ and $>10^{-2}$, respectively), facing even more critically with the problem of their nondetection in the atmosphere and/or at the surface of Io (see section 4.2.3).

[87] Therefore these strong chemical constraints did not allow us to continue to consider H_2S_2 as a possible contributor to the 3.92 μm band in the Marduk spectrum.

4.3. Reddish Material

[88] An intriguing point is the good correlation we found between the area displaying the 3.92 μm absorption band in the NIMS data and the low albedo reddish deposit south of the Marduk volcanic center, as seen in the SSI images (Figure 2). This deposit is linked with recent (post Voyager) plumes still active after the G2 observation [McEwen et al., 1998]. The red coloration is assumed by several authors to be mainly due to S_4 radicals (with some contribution from the yellow-green S_3 radical) emitted by the volcano [Zolotov and Fegley, 1998b] or formed either by atmospheric photochemistry or by surface reaction of abundant S_2 [Moses et al., 2002a; Spencer et al., 2000; McEwen et al., 1998]. The fan-tail shape of the deposit indicates that the plume was probably overpressured, a condition that favors the formation of S_n radicals ($n \geq 3$), but also of several chlorine molecules, including ClS_2 , Cl_2S , Cl_2SO and Cl_2SO_2 [Fegley and Zolotov, 2000; M. Zolotov, Washington University, personal communication, 2001]. In particular, Cl_2S (sulfur dichloride), one of the most abundant chlorine molecules at high pressure (0.1%–1% when Cl dominates over Na + K), is known to be dark red in the liquid phase. Although we have not yet succeeded in measuring its visible spectrum in the solid state, this coloration is clearly retained in the solid phase. This leads us to suggest that the presence of this molecule, probably also trapped within the SO_2 frost, may be an alternative (or competing) explanation for the reddish coloration of some volcanic deposits. Unfortunately this molecule did not have bands strong enough in the NIMS range to be detectable (Rodriguez and Schmitt, submitted manuscript, 2003). Laboratory visible spectra of solid Cl_2S , S_3 , and S_4 , pure and diluted in SO_2 ice and solid S_8 , are clearly needed to compare with the band shape of Io's "red" absorption feature and to assess the absolute and relative abundances of these molecules.

[89] Cl_2S exposed to solar radiation has a photolysis rate constant of only 3.5 hours at Io's surface ($\lambda < 465$ nm, $J \approx 8 \times 10^{-5} \text{ s}^{-1}$). This value is already 2–3 orders of magnitude larger than for S_4 (2.6 min) and S_3 (24 s) [Moses et al., 2002a, 2002b] but not large enough to account for the "years to decades" fading time of the red material [McEwen et al., 1998]. The SO_2 ice matrix cannot efficiently protect Cl_2S against photolysis. However, it is highly probable that a significant amount of sulfur is mixed with SO_2 ($\text{S}_8/\text{SO}_2 \approx 3$ –10% for O/S = 1–1.5 assuming most S_2 is converted to octosulfur at the surface [Zolotov and Fegley, 1998b]). The photons up to 400–420 nm are then almost completely absorbed by S_8 but progressively less efficiently at higher wavelengths [Douté et al., 2001]. We ran a simple modeling, assuming that all solar photons not absorbed by sulfur mixed with SO_2 can dissociate Cl_2S with an efficiency of 1 below 400 nm, decreasing linearly to 0 at 465 nm. This model gives an average photolysis rate of diluted Cl_2S reduced by about a factor of 50–100 compared to unshielded molecules. In addition sulfur reduces the penetration depth of the "destructive photons" compared to the photons that induce the red color (absorbed between ~500 and 650 nm [Geissler et al., 1999]). So the Cl_2S molecules trapped below some depth (~0.1 mm) in the $\text{S}_8:\text{SO}_2$ deposit might be well protected against photolysis (dissociation rate possibly divided by 1,000–10,000) while they are still able to contribute to the visible absorption producing the red color.

[90] In comparison S_3 radicals, although similarly protected by sulfur, are 500 times more sensitive to dissociation ($J \approx 4 \times 10^{-2} \text{ s}^{-1}$, 350 nm $< \lambda < 455$ nm). S_4 radicals trapped in a mixture of SO_2 and S_8 (or in pure solid sulfur) are also much more sensitive to photolysis as their photo-dissociation rate ($J \approx 6.4 \times 10^{-3} \text{ s}^{-1}$, 425 nm $< \lambda < 575$ nm) is 80 times larger than Cl_2S and their photolysis range is at much higher wavelength. Between 500 and 575 nm S_8 did not shield S_4 efficiently. A reduction by only a factor of 2 is found for their photolysis rate. In addition, the depth of S_4 photolysis is about the same as the absorption depth of the photons inducing the red color (same photons!). So even if the S_4 radicals can easily reform from their photolysis products (S , S_2 , and S_3), every radical should do this more than 10^5 to 10^6 times to survive over a few years! On the other hand, the Cl_2S molecules protected in the under-layer need to reform at most a few times (but not necessary if the protection factor is >5000) to produce a time scale of red color fading compatible with observations. In addition to the direct recombination of the dissociation products of Cl_2S (SCl and Cl) [Moses et al., 2002b, reaction R357] other recombination cycles of Cl_2S exist which use only a single ubiquitous SO_2 molecule (reactions R340 + R443) or less probably one S (R228 + R440) or S_2 radical (R277 + R347 + R294) trapped near the photolysis products. But there are also a number of ways to lose Cl and SCl by reaction with other trapped atoms or molecules [Moses et al., 2002b].

[91] In conclusion, Cl_2S has the required properties to provide a strongly challenging explanation (over S_4 and S_3) for the reddish color of the Marduk deposits (and possibly others) and its progressive fading with time [McEwen et al., 1998]. The very high dissociation rates of S_3 and S_4 are

crucial issues to be solved if these radicals are indeed at the origin of some red deposits.

5. Summary

[92] On the basis of purely spectroscopic arguments, four molecules (Cl_2SO_2 , ClSO_2 , H_2S and H_2S_2) have been selected as the only potential candidates to explain the $3.92\ \mu\text{m}$ absorption band observed in the reddish area south of the Marduk volcanic center. Their abundances and physical states have been inferred from the NIMS observation using radiative transfer modeling. Formation, condensation and destruction scenarios, taking into account the existing volcanic and atmospheric chemical models completed with some chemical and thermodynamical data, have been proposed for each of these molecules in order to link their state at the surface with volcanic plume physical conditions and abundances. Their analysis allowed us to accept or reject the various proposed scenarios.

[93] The major conclusions reached in this study are summarized in the following:

[94] 1. Cl_2SO_2 is our favorite candidate. An excellent fit of the $3.92\ \mu\text{m}$ band is obtained for a millimeter thick layer of 1% Cl_2SO_2 diluted in solid SO_2 and covering a similar mixture but strongly depleted in Cl_2SO_2 ($<0.1\%$). Although the Cl_2SO_2 gas mole fraction ($\sim 10^{-6}$) necessary to condense this enriched layer may be compatible with volcanic abundances under special but still plausible vent conditions, the issue of the destiny of the major part of SO_2 did not allow us to further support this differentiation scenario. We rather strongly favor a formation process of this molecule by direct reaction of abundant atmospheric Cl atoms on condensing SO_2 ice. This heterogeneous reaction may occur either on growing SO_2 plume particles or on condensing SO_2 frost at Io's surface, depending on the effective process of SO_2 condensation at Marduk. Favorable conditions for abundant Cl_2SO_2 formation are met only for Cl-rich volcanic eruptions (i.e., for $[\text{Cl} - (\text{Na} + \text{K})]/\text{S} > 0.015$). This was probably the case at Marduk. Once at the surface Cl_2SO_2 should be efficiently protected from UV destruction by a small amount of S_8 mixed with SO_2 ice. Detailed laboratory experiments to demonstrate and quantify the formation of Cl_2SO_2 by direct reaction of Cl atoms on cold SO_2 surfaces are necessary to validate this scenario.

[95] 2. ClSO_2 is a potential alternative candidate as its three main combination bands might fit three bands (including the $3.92\ \mu\text{m}$ one) observed in Marduk's NIMS spectrum. However, the lack of laboratory data did not allow us to resolve this question. ClSO_2 may be easier to produce in substantial amounts by heterogeneous reaction as it appears to be the intermediate product toward the eventual formation of Cl_2SO_2 , but recent unpublished experiments seem to be at variance with this fact. On the other hand ClSO_2 is much less stable and might need a larger abundance ($\sim 2 - 15\%$), and thus a large volcanic Cl/S ratio, to fit the NIMS band strength. Some condition dependent equilibrium between the abundances of Cl_2SO_2 and ClSO_2 may possibly occur but at the present stage in this study we distinctly favor Cl_2SO_2 over ClSO_2 . Spectral and chemical studies of these molecules are urgently needed.

[96] 3. H_2S in the form of a submicron thin layer of pure ice (phase II) condensed on top of SO_2 ice also well fits the observed NIMS band. However, even at the lowest allowed temperature (103.6 K), the persistence of such a thin layer over months at Io's surface is highly improbable. Therefore H_2S can be safely discarded from being the $3.92\ \mu\text{m}$ absorber. However, H_2S diluted in SO_2 ice might be present at a maximum concentration of 0.01% and marginally contribute to the spectrum around $3.85\ \mu\text{m}$. But no positive proof exists.

[97] 4. H_2S_2 diluted at low concentration (0.01% – 0.1%) in SO_2 ice might possibly fit the band position, but the lack of laboratory data did not allow any spectral conclusion to be made. As for Cl_2SO_2 , no strong differentiation can occur otherwise unsolvable problems arise with SO_2 . The very strong H/S ratio ($>10^{-2}$) and the unlikely abundances of the other hydrogenated molecules implied by the H_2S_2 abundance allows us to exclude this molecule as a possible contributor to the $3.92\ \mu\text{m}$ band.

6. Conclusion

[98] Two major questions raised by the local identification of Cl_2SO_2 (with maybe some ClSO_2) near Marduk, and possibly at a few other local spots, are: Why are these molecules not observed in all the volcanic deposits? What determines their formation and their abundance?

[99] First, the heterogeneous formation of these chlorine molecules should be efficient only on condensing SO_2 . If during an eruption SO_2 did not condense on the plume particles, the reaction can only occur on condensing frost at the surface. In addition, their destruction by UV or their burial by SO_2 frost is effective where the diurnal sublimation-recondensation cycle segregates these molecules. All this restricts their observability to fresh volcanic deposits.

[100] Second, the atmospheric abundance of atomic Cl mainly and strongly depends on the relative elemental abundances of Cl compared to Na and K. Typical abundances of Cl atoms relative to SO_2 vary from 0.001% to 13% for $[\text{Cl} - (\text{Na} + \text{K})]/\text{S}$ ratios varying from -0.1 to 0.1 [*Moses et al.*, 2002b]. An excess of a few hundredth of the elemental ratio Cl/S over $(\text{Na} + \text{K})/\text{S}$ is then enough to obtain abundant atomic Cl in the atmosphere. But this is probably a rather uncommon volcanic composition that may occur only at some places on Io.

[101] Finally, the $3\text{-}\sigma$ detection limit for Cl_2SO_2 diluted in solid SO_2 (with the $3.92\ \mu\text{m}$ band) is of the order of 0.2%, just a factor of 5 below the abundance derived near Marduk. So Cl_2SO_2 would be difficult to observe in other regions of Io if it were just a few times less abundant than at Marduk. At concentrations below 0.2% none of the few IR-active chlorine molecules (Cl_2SO_2 , ClSO_2 , Cl_2SO , ClO , Cl_2O , ...) in the solar spectrum might be observable by NIMS. Only spectroscopic observations in the thermal IR (emission features) might reveal the presence of some of the most abundant Cl-bearing volcanic molecules such as NaCl, KCl, ClS_2 or Cl_2S . NaCl has very recently been observed in the atmosphere of Io and a mean volcanic flux in the range 0.3–1.3% relative to SO_2 has been inferred [*Lellouch et al.*, 2003]. NaCl having a very low vapor pressure it might differentiate from SO_2 and then be locally present at much higher concentrations at the surface.

[102] In order to solve all the issues raised by the identification of Cl_2SO_2 (and possibly ClSO_2), additional laboratory experiments on the spectroscopic properties of several molecules (ClSO_2 , Cl_2S , S_n , ...) and on the heterogeneous formation of Cl_nSO_2 ($n = 1, 2$) are needed. A series of experiments have already been initiated at LPMA (L. Schriver and A. Schriver, Université P. & M. Curie, Paris, 2002). New chemical models including more realistic condensation and transport processes in volcanic plume conditions are also needed to incorporate the heterogeneous reactions occurring on plume particles. Finally, the search of new areas unambiguously displaying the $3.92 \mu\text{m}$ band, with possibly some associated bands, should help to determine the possible presence of ClSO_2 and its contribution to the bands.

[103] **Acknowledgments.** Many thanks to Olivier Brissaud for his technical help during the laboratory experiments. We wish to gratefully thank Bob Carlson (NIMS's P.I.) for his confidence when he proposed to our group to work on the Io NIMS data. We also would like to thank Bob Mehlan, Sylvain Douté, and Larry Soderblom for their help with the NIMS data and for interesting discussions. We are grateful to Mikhail Zolotov for performing specific chemical calculations on the Cl_2SO_2 issue. We also had very fruitful discussions with Mikhail, Julie Moses, and Bruce Fegley, from which emerged the idea of heterogeneous formation (by J.M.). The judicious comments from the reviewers especially helped us to improve our demonstration of the possibility of "reactions on volcanic plume." We acknowledge CNES (Solar System Program) and the French "Programme National de Planétologie" of INSU (CNRS) for their financial supports. This work has been performed in the framework of the NIMS/Galileo Team.

References

- Anderson, A., O. S. Binbrek, and H. C. Tang, Raman and infrared study of the low temperature phase of solid H_2S and D_2S , *J. Raman Spectrosc.*, **6**, 213–220, 1977.
- Bahou, M., S.-F. Chen, and Y.-P. Lee, Production and infrared absorption spectrum of ClSO_2 in matrices, *J. Phys. Chem. A*, **104**, 3613–3619, 2000.
- Brown, R. A., Optical line emission from Io, in *Exploration of the Planetary System*, edited by A. Woszczyk and C. Iwaniszewska, pp. 527–531, D. Reidel, Norwell, Mass., 1974.
- Carlson, R., P. R. Weissman, W. D. Smythe, J. C. Mahoney, and the NIMS Science and Engineering Teams, Near infrared spectrometer experiment on Galileo, *Space Sci. Rev.*, **60**, 457–502, 1992.
- Carlson, R., et al., The distribution of sulfur dioxide and other infrared absorbers on the surface of Io, *Geophys. Res. Lett.*, **24**, 2479–2482, 1997.
- Cataldo, V., and L. Wilson, Volcanic eruption plumes on Io: SO_2 condensation on tiny glassy volcanic particles, *Lunar Planet. Sci.*, **XXX**, 1246, 1999.
- Dahmani, R., and R. Khanna, H_2O on Io? IR spectra of $\text{SO}_2/\text{H}_2\text{O}$ mixed ices in the $5000\text{--}450 \text{ cm}^{-1}$ region, *Astron. Space Sci.*, **236**, 125–133, 1996.
- Douté, S., and B. Schmitt, A multi-layer bidirectional reflectance model for the analysis of planetary surface hyperspectral images at visible and near infrared wavelengths, *J. Geophys. Res.*, **103**, 31,367–31,389, 1998.
- Douté, S., B. Schmitt, R. Lopes-Gautier, R. Carlson, L. Soderblom, J. Shirley, and the Galileo NIMS Team, Mapping SO_2 frost on Io by the modeling of NIMS hyperspectral images, *Icarus*, **149**, 107–132, 2001.
- Douté, S., R. Lopes, L. W. Kamp, R. Carlson, W. D. Smythe, B. Schmitt, and the Galileo NIMS Team, Dynamics and evolution of SO_2 gas condensation around Prometheus-like volcanic plumes on Io as seen by the Near Infrared Mapping Spectrometer, *Icarus*, **158**, 460–482, 2002.
- Fanale, F. P., R. H. Brown, D. Cruikshank, and R. Clark, Significance of absorption features in Io's IR reflectance spectrum, *Nature*, **280**, 761–763, 1979.
- Fegley, B., and M. Y. Zolotov, Chemistry of sodium, potassium, and chlorine in volcanic gases on Io, *Icarus*, **148**, 193–210, 2000.
- Feldman, P. D., T. B. Ake, A. F. Berman, H. W. Moos, D. J. Sahnou, D. F. Strobel, H. A. Weaver, and P. R. Young, Detection of chlorine ions in the Far Ultraviolet Spectroscopic Explorer spectrum of the Io plasma torus, *Astrophys. J.*, **554**, L123–L126, 2001.
- Ferraro, J. R., G. Sill, and U. Fink, Infrared intensity measurements of cryodeposited thin films of NH_3 , NH_4HS , H_2S and assignments of absorption bands, *Appl. Spectrosc.*, **34**, 525–533, 1980.
- Geissler, P., A. S. McEwen, L. Keszthelyi, R. M. C. Lopes-Gautier, J. Granahan, and D. P. Simonelli, Global color variations on Io, *Icarus*, **140**, 265–282, 1999.
- Glaze, L. S., and S. M. Baloga, Stochastic-ballistic eruption plumes on Io, *J. Geophys. Res.*, **105**, 17,579–17,588, 2000.
- Hanel, R. A., B. J. Conrath, D. E. Jennings, and R. E. Samuelson, Objects without substantial atmospheres, in *Exploration of the Solar System by Infrared Remote Sensing, Planet. Sci. Ser.*, vol. 7, chap. 6.5, pp. 299–306, Cambridge Univ. Press, New York, 1992.
- Hapke, B. W., Io's surface and environs: A magmatic-volatile model, *Geophys. Res. Lett.*, **6**, 799–802, 1979.
- Hapke, B. W., The surface of Io: A new model, *Icarus*, **79**, 56–74, 1989.
- Haynes, D. R., N. J. Tro, and S. M. George, Condensation and evaporation of H_2O on ice surfaces, *J. Phys. Chem.*, **96**, 8502–8509, 1992.
- Honig, R. E., and H. O. Hook, Vapor pressure data for some common gases, *RCA Rev.*, **21**, 360–368, 1960.
- Howell, R. R., D. B. Nash, T. R. Geballe, and D. P. Cruikshank, High-resolution infrared spectroscopy of Io and possible surface materials, *Icarus*, **78**, 27–37, 1989.
- Johnson, R. E., Polar "caps" on Ganymede and Io revisited, *Icarus*, **128**, 469–471, 1997.
- Khanna, R. K., J. C. Pearl, and R. Dahmani, Infrared spectra and structure of solid phases of sulfur trioxide: Possible identification of solid SO_3 on Io's surface, *Icarus*, **115**, 250–257, 1995.
- Küppers, M., and N. M. Schneider, Discovery of chlorine in the Io torus, *Geophys. Res. Lett.*, **27**, 513–516, 2000.
- Lellouch, E., M. Belton, I. de Pater, S. Gulkis, and T. Encrenaz, Io's atmosphere from microwave detection of SO_2 , *Nature*, **346**, 639–641, 1990.
- Lellouch, E., G. Paubert, J. I. Moses, N. M. Schneider, and D. F. Strobel, Volcanically-emitted sodium chloride as a source for Io's neutral clouds and plasma torus, *Nature*, **421**, 45–47, 2003.
- Lester, D. F., L. M. Trafton, T. F. Ramseyer, and N. I. Gaffney, Discovery of a second narrow absorption feature in the near infrared spectrum of Io, *Icarus*, **98**, 134–140, 1992.
- Lide, D. R., Fluid properties: Vapor pressure of inorganic compounds, in *Handbook of Chemistry and Physics*, 71th ed., pp. 6-50–6-54, CRC Press, Boca Raton, Fla., 1990.
- McEwen, A. S., et al., Active volcanism on Io as seen by Galileo SSI, *Icarus*, **135**, 181–219, 1998.
- Moore, M. H., Studies of proton-irradiated SO_2 at low temperatures: Implications for Io, *Icarus*, **59**, 114–128, 1984.
- Moses, J. I., and D. B. Nash, Phase transformations and spectral reflectance of solid sulfur: Can metastable sulfur allotropes exist on Io?, *Icarus*, **89**, 277–304, 1991.
- Moses, J., M. Y. Zolotov, and B. Fegley, Photochemistry of a volcanically driven atmosphere on Io: Sulfur and oxygen species from a Pele-type eruption, *Icarus*, **156**, 76–106, 2002a.
- Moses, J., M. Y. Zolotov, and B. Fegley, Alkali and chlorine photochemistry in volcanically driven atmosphere on Io, *Icarus*, **156**, 107–135, 2002b.
- Nash, D. B., Infrared reflectance spectra of Na_2S with contaminant Na_2CO_3 —Effects of adsorbed H_2O and CO_2 and relation to studies of Io, *Icarus*, **74**, 365–368, 1988.
- Nash, D. B., and B. H. Betts, Ices on Io—Composition and texture, in *Solar System Ices*, edited by B. Schmitt et al., *Astrophys. Space Sci. Lib.*, vol. 227, pp. 607–637, Kluwer Acad., Norwell, Mass., 1998.
- Nash, D. B., and R. R. Howell, Hydrogen sulfide on Io: Evidence from telescopic and laboratory infrared spectra, *Science*, **244**, 454–457, 1989.
- Nash, D. B., and R. M. Nelson, Spectral evidence for sublimates and adsorbates on Io, *Nature*, **280**, 763–766, 1979.
- Nash, D. B., F. P. Fanale, and R. M. Nelson, SO_2 frost: UV-visible reflectivity and Io surface coverage, *Geophys. Res. Lett.*, **7**, 655–668, 1980.
- Nelson, R. M., and W. D. Smythe, Spectral reflectance of solid sulfur trioxide $0.25\text{--}5.2 \mu\text{m}$: Implications for Jupiter's satellite Io, *Icarus*, **66**, 181–187, 1986.
- Pearl, J. C., A review of Voyager IRIS results on Io, *Eos Trans. AGU*, **69**, 394, 1988.
- Post, B., R. S. Schwartz, and I. Fankuchen, The crystal structure of solid sulfur dioxide, *Acta Crystallogr.*, **5**, 372–374, 1952.
- Quirico, E., S. Douté, B. Schmitt, C. de Bergh, D. P. Cruikshank, T. C. Owen, T. R. Geballe, and T. L. Roush, Composition, physical state and distribution of ices at the surface of Triton, *Icarus*, **139**, 159–178, 1999.
- Reding, F. P., and D. F. Hornig, Vibrational spectra of molecules and complex ions in crystals, X. H_2S and D_2S , *J. Chem. Phys.*, **27**, 1024–1030, 1957.
- Roesler, F. L., et al., Far-ultraviolet imaging spectroscopy of Io's atmosphere with HST/STIS, *Science*, **283**, 353–357, 1999.
- Russell, C. T., and M. G. Kivelson, Evidence for sulfur dioxide, sulfur monoxide and hydrogen sulfide in the Io exosphere, *J. Geophys. Res.*, **106**, 33,267–33,272, 2001.

- Salama, F., L. J. Allamandola, F. C. Witteborn, D. P. Cruikshank, S. A. Sandford, and J. D. Bregman, The 2.5–5.0 μm spectra of Io: Evidence for H₂S and H₂O frozen in SO₂, *Icarus*, *83*, 66–82, 1990.
- Salama, F., L. J. Allamandola, S. A. Sandford, J. D. Bregman, F. C. Witteborn, and D. P. Cruikshank, Is H₂O present on Io? The detection of a new strong band near 3590 cm^{-1} (2.79 μm), *Icarus*, *107*, 413–417, 1994.
- Sandford, S. A., and L. J. Allamandola, The condensation and vaporization behavior of ices containing SO₂, H₂S, and CO₂: Implications for Io, *Icarus*, *106*, 478–488, 1993.
- Sandford, S. A., F. Salama, L. J. Allamandola, L. M. Trafton, D. F. Lester, and T. F. Ramseyer, Laboratory studies of the newly discovered infrared band at 4705.2 cm^{-1} (2.125 microns) in the spectrum of Io: The tentative identification of CO₂, *Icarus*, *91*, 125–144, 1991.
- Schianouchi, T., *NIST Chemistry WebBook, NIST Stand. Ref. Database 69*, edited by W. G. Mallard and P. J. Linstrom, Natl. Inst. of Stand. and Technol., Gaithersburg, Md., 2000. (Available at <http://webbook.nist.gov>)
- Schmitt, B., and S. Rodriguez, Tentative identification of a chlorine molecule at Io's surface, *Bull. Am. Astron. Soc.*, *32*, abstract 29.10, 2000.
- Schmitt, B., and S. Rodriguez, Tentative identification of local deposits of Cl₂SO₂ at Io's surface, *Lunar Planet. Sci.*, *XXXII*, 1710, 2001.
- Schmitt, B., C. De Bergh, E. Lellouch, J. P. Maillard, A. Barbe, and S. Douté, Identification of three absorption bands in the 2- μm spectrum of Io, *Icarus*, *111*, 79–105, 1994.
- Schmitt, B., E. Quirico, F. Trotta, and W. Grundy, Optical properties of ices from UV to infrared, in *Solar System Ices*, edited by B. Schmitt et al., *Astrophys. Space Sci. Lib.*, vol. 227, pp. 199–240, Kluwer Acad., Norwell, Mass., 1998.
- Schmitt, B., E. Lellouch, S. Douté, H. Feuchtgruber, C. de Bergh, and J. Crovisier, High resolution infrared spectra (2.4–5.3 μm) of the surface of Io with ISO: The physical state of solid SO₂, *Icarus*, in preparation, 2003.
- Smythe, W. D., R. M. Nelson, and D. B. Nash, Spectral evidence for SO₂ frost or adsorbate on Io's surface, *Nature*, *280*, 766, 1979.
- Soderblom, L. A., K. J. Becker, T. L. Becker, R. W. Carlson, A. G. Davies, J. S. Kargel, R. L. Kirk, R. C. Lopes-Gautier, W. D. Smythe, and J. M. Torson, Deconvolution of Galileo NIMS day-side spectra of Io into thermal, SO₂, and non-SO₂ components, *Lunar Planet. Sci.*, *XXX*, 1901, 1999.
- Spencer, J. R., P. Sartoretti, G. E. Ballester, A. S. McEwen, J. T. Clarke, and M. A. McGrath, The Pele plume (Io): Observations with the Hubble Space Telescope, *Geophys. Res. Lett.*, *24*, 2471–2474, 1997.
- Spencer, J. R., K. L. Jessup, M. A. McGrath, G. E. Ballester, and R. Yelle, Discovery of gaseous S₂ in Io's Pele plume, *Science*, *288*, 1208–1210, 2000.
- Strobel, D. F., and B. C. Wolven, The atmosphere of Io: Abundances and sources of sulfur dioxide and atomic hydrogen, *Astrophys. Space Sci.*, *277*, 271–287, 2001.
- Summer, M. E., and D. F. Strobel, Photochemistry and vertical transport in Io's atmosphere and ionosphere, *Icarus*, *120*, 290–316, 1996.
- Trotta, F., Détermination des constantes optiques des glaces dans l'infrarouge moyen et lointain. Application aux grains du milieu interstellaire et des enveloppes circumstellaires, doctorate thesis, LGGE - Université J. Fourier, Grenoble, France, 1996.
- Wagman, D. D., Sublimation pressure and enthalpy of sublimation of SO₂, Chem. Thermodyn. Data Cent. Rep., Natl. Bur. of Standards, Washington, D. C., 1979.
- Wong, M. C., and R. E. Johnson, A three-dimensional azimuthally symmetric model atmosphere for Io, 1, Photochemistry and the accumulation of a nightside atmosphere, *J. Geophys. Res.*, *101*, 23,243–23,254, 1996a.
- Wong, M. C., and R. E. Johnson, A three-dimensional azimuthally symmetric model atmosphere for Io, 2, Plasma effect on the surface, *J. Geophys. Res.*, *101*, 23,255–23,259, 1996b.
- Zolotov, M. Y., and B. Fegley, Volcanic production of sulfur monoxide (SO) on Io, *Icarus*, *132*, 431–434, 1998a.
- Zolotov, M. Y., and B. Fegley, Volcanic origin of disulfur monoxide (S₂O) on Io, *Icarus*, *133*, 293–297, 1998b.
- Zhang, J., D. B. Goldstein, P. L. Varghese, N. E. Gimelshein, S. F. Gimelshein, and D. A. Levin, Simulation of gas dynamics and radiation in volcanic plumes on Io, *Icarus*, *163*, 182–197, 2003.

S. Rodriguez, Observatoire de Bordeaux, 2 rue de l'Observatoire, B.P. 89, 33270, Floirac, France. (rodriguez@observ.u-bordeaux.fr)

B. Schmitt, Laboratoire de Planétologie de Grenoble (LPG), CNRS-Université J. Fourier, Bâtiment D de Physique, 122 rue de la Piscine, 38041 Grenoble Cedex 9, France. (Bernard.Schmitt@obs.ujf-grenoble.fr)